

Mapping of Holocene River Alluvium along the San Pedro River, Aravaipa Creek, and Babocomari River, Southeastern Arizona

by

Joseph P. Cook, Ann Youberg, Philip A. Pearthree, Jill A. Onken, Bryan J.
MacFarlane, David E. Haddad, Erica R. Bigio, Andrew L. Kowler

*A Report to the
Adjudication and Technical Support Section
Statewide Planning Division
Arizona Department of Water Resources*

**Report accompanies
Arizona Geological Survey Digital Map DM-RM-1
Map Scale 1:24,000 (6 sheets), 76 p.**

Originally issued, July 2009

Version 1.1 released, October 2009

Arizona Geological Survey
416 W Congress St., #100, Tucson, AZ 85701

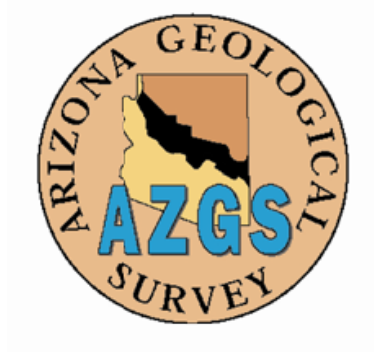


Table of Contents

Introduction	3
• Geologic Mapping Methods	3
• Mapping Criteria	3
• Ages of Deposits	5
Mapping the extent of Holocene alluvium	7
• Field data collection and access	8
• Surficial geologic contacts	8
• Soil Survey mapping	8
• Extent of Holocene River Floodplain Alluvium	16
• Geologic Map versions	17
Soil parameters and age estimates for soils in the southern San Pedro Valley	18
San Pedro River Geology and Geomorphology	22
• Geologic History	22
• Historical Change	23
• Geomorphology	24
• Modern channel conditions	24
Babocomari River Geology and Geomorphology	26
• Geologic History	26
• Historical Change	27
• Geomorphology	27
• Modern channel conditions	28
Aravaipa Creek Geology and Geomorphology	30
• Geologic History	30

• Historical Change	30
• Geomorphology	32
• Modern channel conditions	33
Geoarchaeological Evaluation	34
• Methods	34
• Results	35
List of map units	42
• Surficial units	42
• Other units	42
• Holocene river alluvium	42
• Pleistocene river alluvium	44
• Piedmont alluvium and surficial deposits	45
• Tertiary basin fill alluvium	51
• Bedrock units	54
References	71

Introduction

The purpose of these investigations is to document and map the extent of Holocene channel and floodplain alluvium associated with the San Pedro River and its major tributaries in southeastern Arizona. Mapping done in this study will be used by Arizona Department of Water Resources (ADWR) staff as part of their effort to delineate subflow zones in the San Pedro River Watershed. The Maricopa County Superior Court has requested that ADWR delineate subflow zones associated with the San Pedro River as part of its work in the Gila River water rights adjudication. Geologic mapping is a primary function of the Arizona Geological Survey (AZGS), so in cooperation with ADWR staff we have established procedures and protocols for documenting and mapping the extent of Holocene floodplain alluvium along rivers in Arizona.

Geologic Mapping Methods

The AZGS has been actively involved in mapping surficial deposits in Arizona for the past 20 years. During this time, the AZGS has produced many 1:24,000-scale 7 ½' quadrangle maps with detailed surficial geologic mapping in southern, central and western Arizona. All of these maps differentiate alluvial deposits based on relative age, and most maps separate deposits associated with larger axial drainages (rivers or washes) from local tributary deposits. In the San Pedro Valley, AZGS geologists have mapped fourteen 7 ½' quadrangles at 1:24,000-scale in the past 6 years that cover portions of the San Pedro River (Shipman and Ferguson, 2003; Pearthree, 2003; Youberg et al, 2004; Youberg, 2006; Shipman and Ferguson, 2006; Ferguson et al., 2006; Pearthree et al., 2006; Youberg et al., 2007; Cook et al., 2007; Cook and Spencer, 2008; Spencer, Richard et al., 2008; Spencer, Cook et al, 2008; Pearthree et al, 2009;), and preliminary geologic mapping has been completed for 3 additional quadrangles during the past year (Figure 1). Although most of these mapping efforts were not directed specifically at delineating Holocene floodplain alluvium, they provide information about the distribution of deposits of various ages and from various sources and thus can be used to delineate the extent of Holocene river deposits. Geologic mapping depicted outside of the Holocene river alluvium corridor was compiled from and is consistent with these maps.

Mapping Criteria. Quaternary geologists use several criteria to differentiate and map river and tributary alluvial deposits of different ages. River deposits commonly consist of two fairly distinct phases: channel deposits dominated by sand and gravel, and overbank deposits found on flood plains and terraces that are composed of fine sand, silt and clay with minor gravel. River channel deposits are distinguished from tributary deposits based on the presence of well-rounded pebbles and cobbles composed of diverse rock types derived from upstream areas along the river. Tributary deposits typically have less diversity of rock types, gravel tends to be more angular, and in many areas, tributary deposits have less silt and clay. Overbank deposits associated with the river typically are thicker and more laterally extensive than fine-grained tributary deposits, although deposits of large tributaries may be quite similar to river deposits. Landforms associated with deposits also provide clues to their origin. This is especially important because landforms can be analyzed using topographic information and aerial photos. Slopes of landforms associated with river deposits (the river channel, flood plain and terraces) are typically quite low

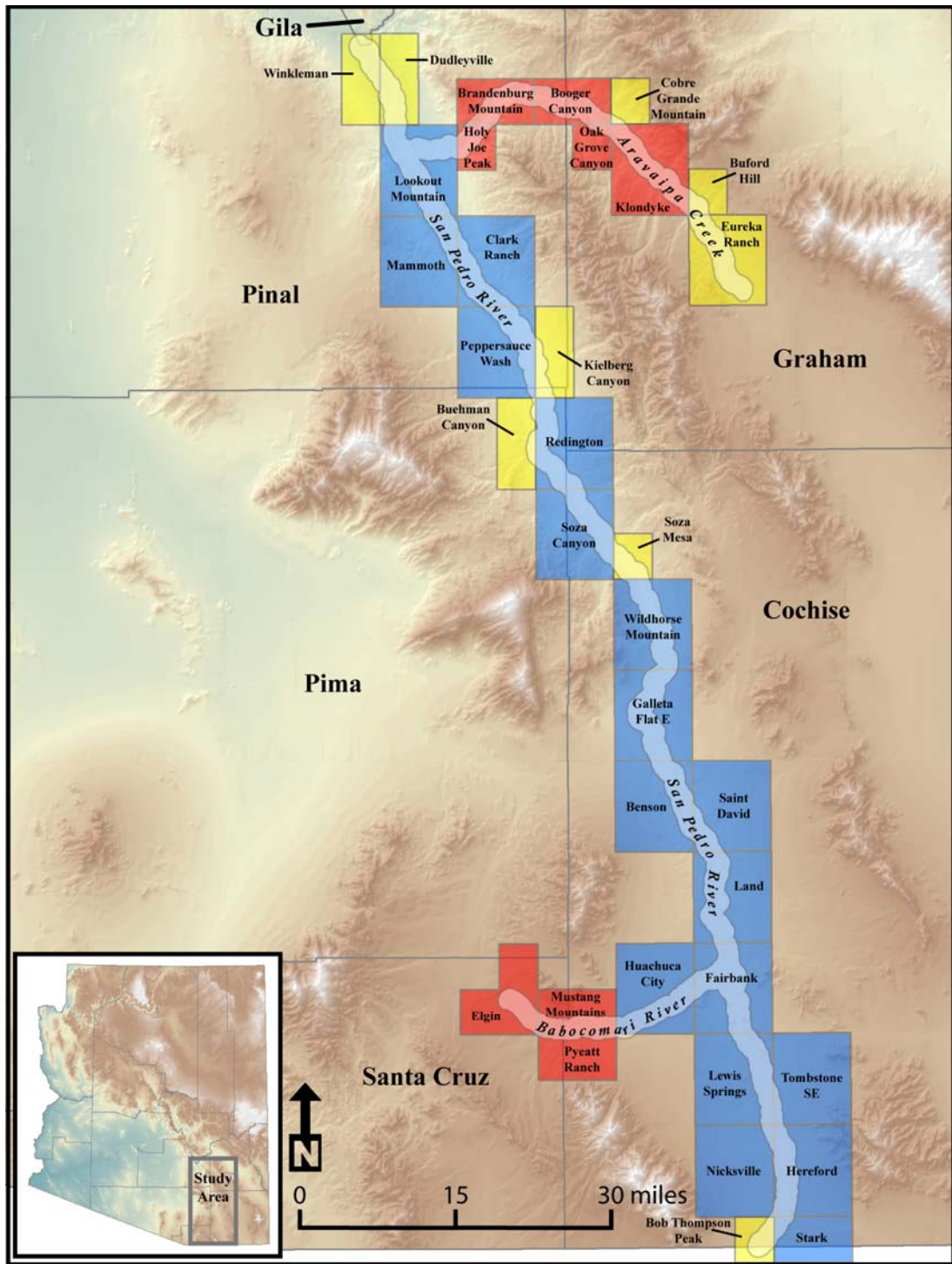


Figure 1. Location map showing the extent of mapping of Holocene floodplain alluvium discussed in this report. The area depicted in the strip maps is shown by white shading. Blue boxes are 7 1/2' quadrangles previously mapped by AZGS geologists. Yellow boxes represent areas which no prior mapping existed and new mapping was conducted for this project. Red boxes are portions of quadrangles not mapped by AZGS geologists from which geologic mapping outside of the Holocene river alluvium was digitized (i.e. USGS or thesis bedrock mapping).

and generally mimic the down-valley slope of the modern river, whereas the gradients of landforms associated with tributary deposits are steeper and generally slope toward the valley axis. Along the river, slopes formed on bedrock and older basin deposits, and reworked sediment derived from them, are steeper yet and slope toward the river.

Deposits and alluvial surfaces associated with them may also be differentiated by age using a variety of criteria (e.g., Gile et al, 1981; McFadden, 1981; Pearthree and Calvo, 1987; NRCS, 2003). In the semiarid southwestern U.S., surface color varies with age because of soil color, vegetation, and rock varnish. Surfaces on piedmont and river deposits of Holocene age typically are light gray to light brown in color (10 YR to 7.5 YR on a soil color chart), reflecting the color of the silt, sand, pebbles and cobbles that make up most of the deposits. Pleistocene surfaces typically have slightly or distinctly reddened color (7.5 YR to 2.5 YR) associated with clay accumulation and oxidation in the near-surface soil, and may be mantled by reddish- or black-coated pebbles and cobbles. Relatively young alluvial surfaces typically retain abundant evidence of the depositional processes that initially shaped them (channels, sand and gravel bars, and swales) whereas older surfaces have been smoothed by local erosion of bars and infilling of swales. Dendritic tributary (joining downstream) drainage patterns are characteristic of older surfaces that are not subject to extensive flooding, and typically older deposits are increasingly more deeply incised and eroded by tributary drainages. Because of this, very old surfaces may be substantially degraded by erosion. The net result of all of these varying surface characteristics is that surfaces of different ages have quite different aspects on the ground and on aerial photographs.

Ages of Deposits. In an area like the San Pedro Valley that has undergone long-term downcutting, older surfaces are relatively higher above active washes. Soil development provides a somewhat more quantitative basis for estimating deposit and alluvial surface ages. Significant soil development begins beneath an alluvial surface after it becomes isolated from active flooding and depositional processes (Gile et al., 1981; Birkeland, 1999). Over thousands to tens of thousands of years, distinct horizons rich in reddened clay (argillic) or calcium carbonate (calcic) develop in soils. Comparison of soil horizon development in surficial deposits in the San Pedro Valley (e.g., NRCS, 2003) with other soil sequences in the western United States is the primary method used to estimate the ages of the different alluvial surfaces (Gile et al, 1981; McFadden, 1981; Machette, 1985; Bull, 1991; Demsey and Pearthree, 1994; P. Camp, NRCS, written comm., 2003). There is uncertainty in age estimates derived from soil characteristics, particularly for river deposits that date approximately to the early Holocene to latest Pleistocene (approximately 5,000 to 20,000 years old).

Where they exist and have been investigated, archaeological sites, paleontological remains, and other dated organic material can provide direct numerical age estimates for Holocene and latest Pleistocene deposits (e.g., Lindsay et al, 1990; Onken and Huckell, 1989). Several archaeological investigations have been conducted of latest Pleistocene Paleoindian sites in the upper San Pedro Valley. These sites include the remains of large mammals such as mammoth and spear points and other human artifacts, indicating the presence of big-game hunters in association with late Pleistocene fauna (Haynes, 1987). Radiocarbon ages obtained from these sites date to about 12,000 years ago (Haynes, 2007) and essentially mark the Pleistocene – Holocene time boundary. Unfortunately, all of the known sites are located along small tributary washes well upslope of the San Pedro River and the deposits cannot be correlated directly to the deposits exposed along the river. Several Holocene-age archaeological features have been

observed in deposits along the Babocomari River. Sites that are buried in Holocene floodplain deposits are Archaic (pre-dating the development of ceramics), probably greater than 2,000 years old (Onken and Huckell, 1989).

AZGS employs a naming scheme for surficial geologic units utilizing a “Qy” and “Qi” designation for Holocene (young) and Pleistocene (intermediate) age deposits respectively. Older Pleistocene deposits are labeled “Qo”, while units spanning early Quaternary to latest Tertiary time are labeled “QT”. Following the Qy, Qi, and Qo designations are numbers. The higher the number the younger the unit relative to other units with the same letter. For example, Qi3 (late Pleistocene) sediments were deposited after Qi1 and Qi2 deposits and before all Qy deposits (Table 1).

	Epoch	Age	AZGS unit name		Relative Age
			river alluvium	piedmont alluvium	
Quaternary ————— Tertiary	Holocene	present day	Qycr	Qyc	young ↓
			Qy4r	Qy3	
			Qy3r		
			Qy2r	Qy2	
		10 Ka	Qy1r	Qy1	
	Pleistocene			Qi3r	Qi3
				Qi2r	Qi2
				Qi1r	Qi1
		2 Ma			Qo
				-----QTa-----	
Pliocene			Tsy	↓ old	

Table 1. Simplified geologic time scale displaying relative ages and naming conventions for Quaternary to late Tertiary age surficial and lithostratigraphic units. All river-deposited units receive an “r” designation while similarly-aged piedmont deposits do not. Descriptions for all map units shown on map sheets 1 through 6 are located in the last section of this report.

Mapping the Extent of Holocene Floodplain Alluvium

Our strategy for mapping Holocene floodplain alluvium involved the following steps:

- 1) compilation of existing geologic mapping in an ArcGIS framework
- 2) re-evaluation of existing mapping using aerial photos and topographic data
- 3) new mapping of Holocene river alluvium where no large-scale geologic mapping had been done previously
- 4) field-checking of the boundaries of Holocene alluvium in various geologic environments along the river, including systematic collection of GPS field points with observations and ground photos (SanPedro_GPSPoints_FieldNotes.xls and digital photos available on accompanying CD)
- 5) revision of map unit boundaries of existing geologic maps
- 6) depiction of all Holocene river alluvium units on 1:24,000-scale strip maps associated with this report

We compiled all of the existing geologic mapping done by the AZGS in San Pedro Valley and evaluated other existing geologic mapping that covers parts of the San Pedro, Babocomari, and Aravaipa drainages. During the past 17 months, we have checked and revised existing AZGS geologic maps that cover the San Pedro and Babocomari Rivers in San Pedro Valley, and have integrated Holocene mapping with new geologic mapping that was done in three 7 ½' quadrangles in the northern San Pedro Valley in the past year. We have completed new mapping along the San Pedro, Babocomari and Aravaipa flood plains where no previous mapping existed (Figure 1). We revised the existing geologic maps based on aerial photo interpretation, topography from 7 ½' quadrangles, 10-meter DEM (USGS, 2008) and LIDAR-based detailed topography along the river, and extensive field investigations, so that they accurately portray the extent of Holocene river alluvium.

Boundaries of Holocene river alluvium were verified through extensive fieldwork and map analyses. We collected GPS points, made field observations, and took ground photos at the lateral margins of Holocene river alluvium at approximately 1-mile spacing along the river. We used standard geologic nomenclature (solid, dashed and dotted lines) to depict the positional uncertainty of the lateral limits of Holocene river alluvium. From the geologic quadrangle maps, we extracted an approximately 2-mile-wide strip geologic map centered on the San Pedro River and major tributaries to depict the extent of Holocene river alluvium (Figure 2). Some geologic mapping outside of the Holocene river alluvium corridor was compiled from older USGS and thesis maps where AZGS mapping does not exist. In all cases, the relationships and extent of Holocene river alluvium and bounding units throughout the mapped area were mapped and field checked as part of this project. Holocene river alluvium is depicted as active channel (unit Qy_cr) and flood channels, low terraces and remnants of Holocene floodplains (Qy₄r – Qy₁r). Holocene river alluvium is bounded by Holocene tributary alluvial fans and channels, Pleistocene alluvial fans and river terraces, eroded basin deposits, and bedrock (Figure 3). The 2-mile-wide strip was chosen to illustrate the nature of the bounding limits of Holocene river alluvium, because the certainty of the limit of Holocene river alluvium is strongly dependent on the nature of the bounding geologic units.

Field Data Collection and Access. We collected field data on the lateral limits of Holocene river alluvium every mile where access was permitted, and made observations at other sites as needed. Data collected include GPS waypoints, ground photos, and field notes. River access generally is good, but private property limited field data collection in a few areas. Throughout steep-walled canyon reaches such as Aravaipa Canyon, GPS reception may be weak to nonexistent due to obstruction of satellite signal or reflected signals from canyon walls, and in the best cases positional uncertainty is relatively large. In these reaches GPS control points were recorded where signal was available as near as possible to the Holocene river alluvium boundary. Detailed notes and photos were recorded for these locations and map linework was compiled using a combination of field collected data and high resolution aerial photography (Figure 4, for example).

Geologic Contacts. We use 3 different line types to delineate the margins of Holocene river alluvium depending on the clarity of the contact.

- 1) Solid line – The contact between Holocene alluvium and the bounding geologic unit is clear and associated with a distinct topographic feature. We find these clearly defined, accurately located contacts associated with bedrock hillslopes, fairly steep scarps or terrace risers cut into older deposits, distinct margins of small active alluvial fans or talus slopes, or boundaries of small entrenched tributary channels (Figures 4, 5, and 6). We estimate that line location is accurate to within 50 feet (± 25 ft).
- 2) Dashed line – The contact between Holocene river alluvium and the bounding geologic unit is subtle or gradational and more difficult to confidently identify on the ground. These subtle contacts are commonly found at the boundaries between Holocene river alluvium and Holocene fine-grained tributary fans (Figures 7 and 8). Slopes in the distal portions of these larger fans are relatively low and little different from floodplain slopes, and deposits from both sources are typically quite fine-grained. In some areas, vegetation changes at the contact between floodplain and distal fan deposits, but in other areas obvious vegetation changes do not appear to correspond with these contacts and may be reflecting other variables such as depth to water. Dashed line boundaries are also commonly located within historically plowed fields. We estimate that line location is accurate to within 100 feet (± 50 ft).
- 3) Dotted line – The contact between Holocene river alluvium and the bounding geologic unit (typically, tributary fans or slightly higher river terraces) has been thoroughly obscured by anthropogenic activity and must be inferred using other information. In these areas, we place the lateral boundary of Holocene floodplain alluvium based on topography if it has not been obliterated, interpretation of older aerial photos that pre-date disturbance, and soil survey information. There is greater uncertainty in the location of these contacts, and occupation of these sites in the field does not substantially improve positional uncertainty (Figure 9, 10, and 11). Dotted line boundary location is probably accurate to within 500 feet (± 250 ft) depending on level of disturbance.

Soil Survey Mapping. We have utilized published soil survey maps that cover part of Cochise County (NRCS, 2003; P. Camp, written comm., 2003) to check our map interpretations and to assist in assigning Holocene or Pleistocene age estimates to deposits found along the river. In general, soil map units outline the extent of Holocene alluvium, but a number of soil map units include both Holocene river and tributary alluvium. Thus, we did not rely primarily on soil survey maps to delineate the extent of Holocene river alluvium, and rather are using the geologic

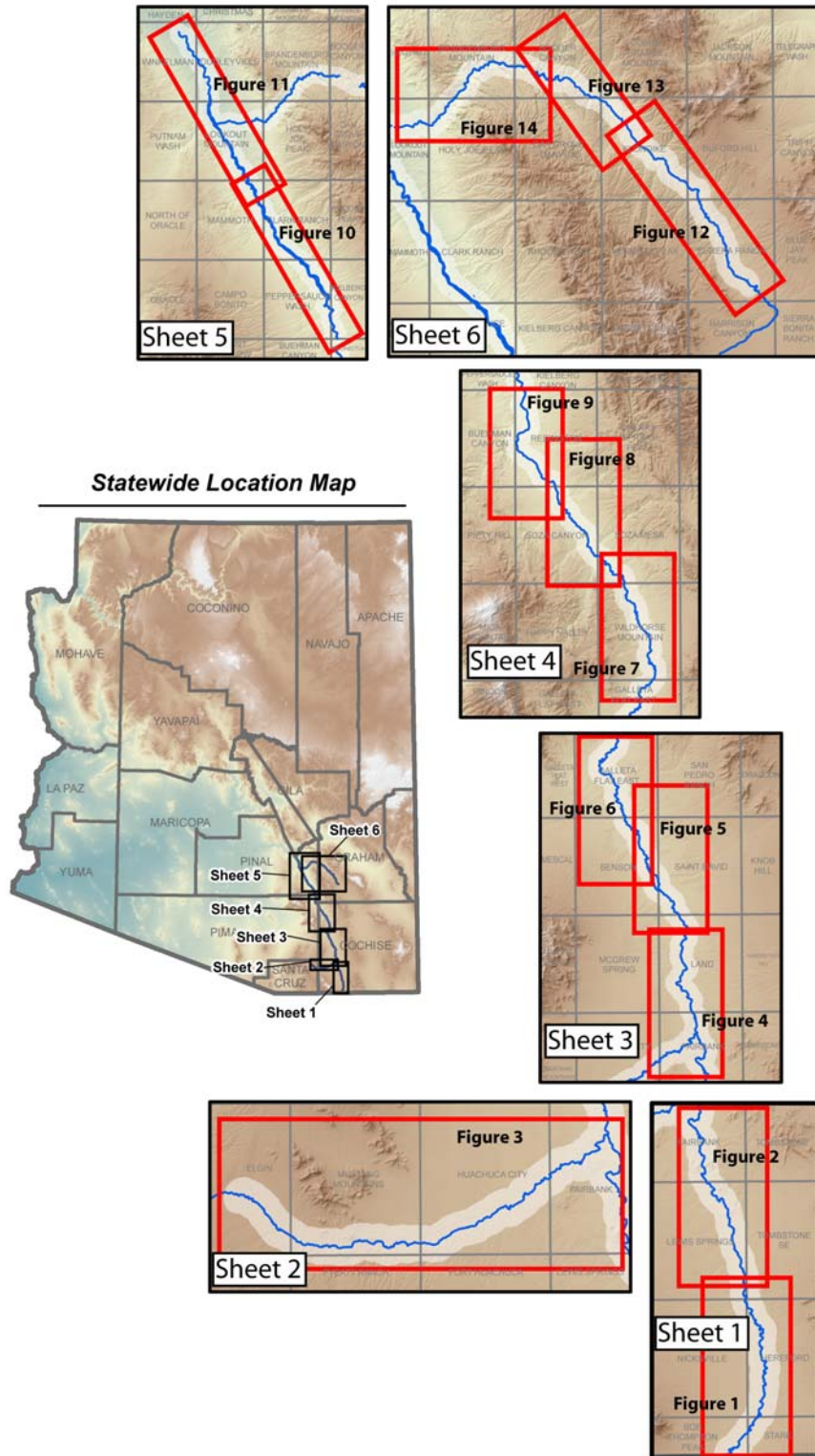


Figure 2. Schematic diagram depicting numbering of map sheets 1 through 6 (black boxes). Individually numbered sheet figures (red boxes) often span multiple 7 1/2' USGS quadrangle maps. Overlap of sheet figures is intentional to ensure complete coverage of mapped areas.

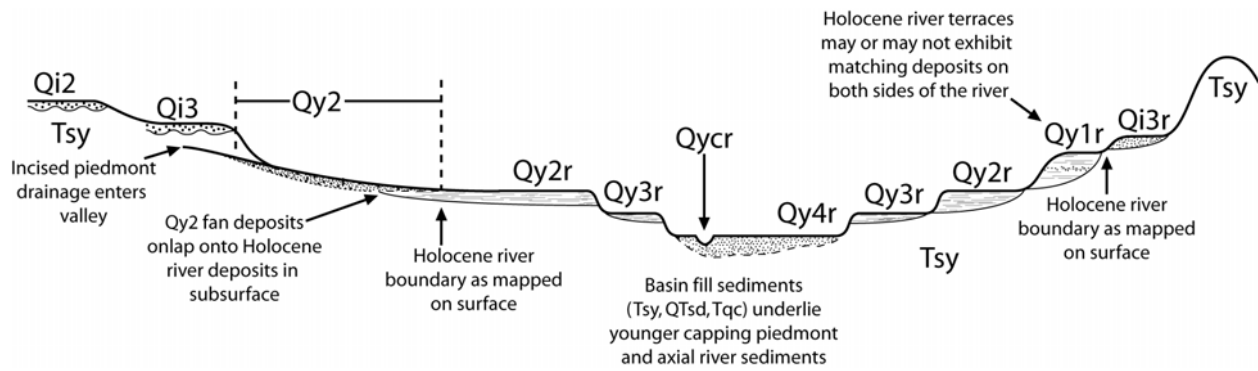


Figure 3. Generalized cross section of geomorphic relationships between Tertiary basin fill (T_{sy}), Pleistocene piedmont and river (Q_{in} and Q_{inr} units), and Holocene piedmont and river (Q_{yn} and Q_{ynr} units) deposits.



Figure 4. Map of bedrock-bounded Holocene floodplain alluvium, just south of Charleston near the northern edge of the Lewis Springs 7 1/2' quadrangle.



Figure 5. Ground photo of a railroad grade near the base of a bedrock hillslope. The limit of Holocene floodplain alluvium is at the base of the railroad grade.

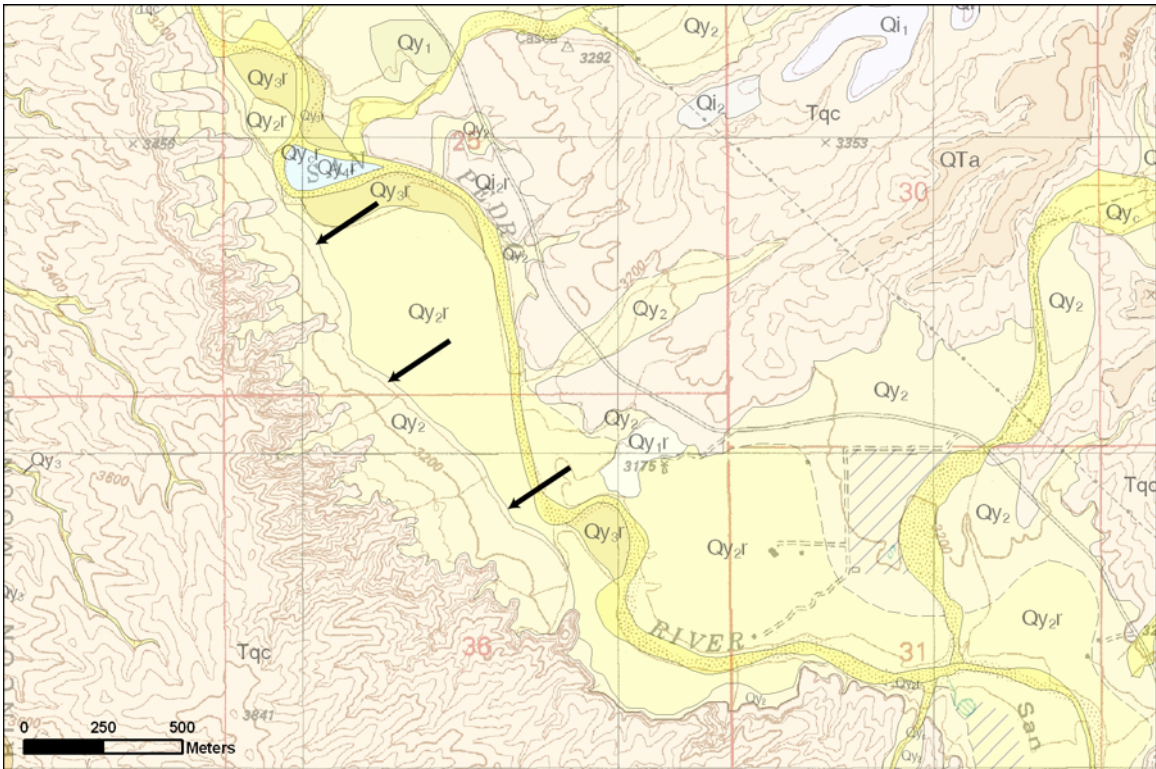
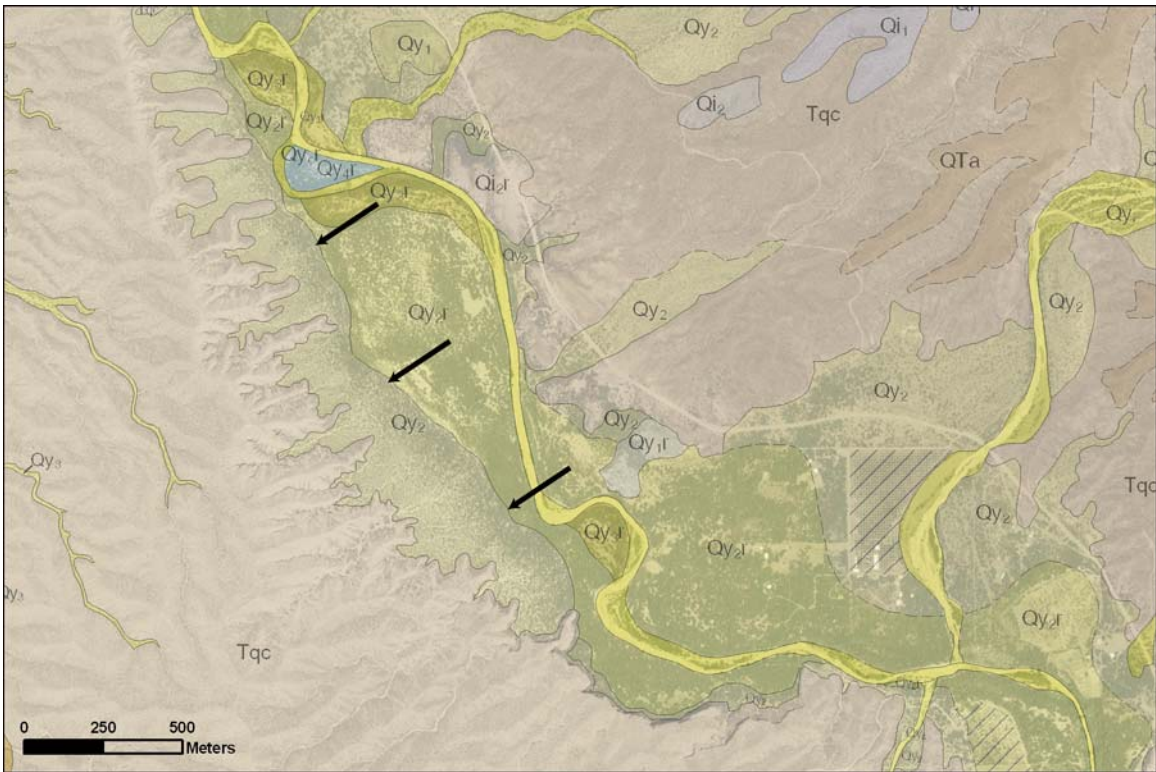


Figure 6. Map of short, steep fans located at the base of tall Quiburis basin fill bluffs. The toe of the fans ends abruptly and can be accurately pinpointed in the field and on aerial photos.



Figure 7. Ground photo of the slope break between Holocene floodplain alluvium (Qyr) and small tributary fans derived from erosion of the St. David Formation (Qys).

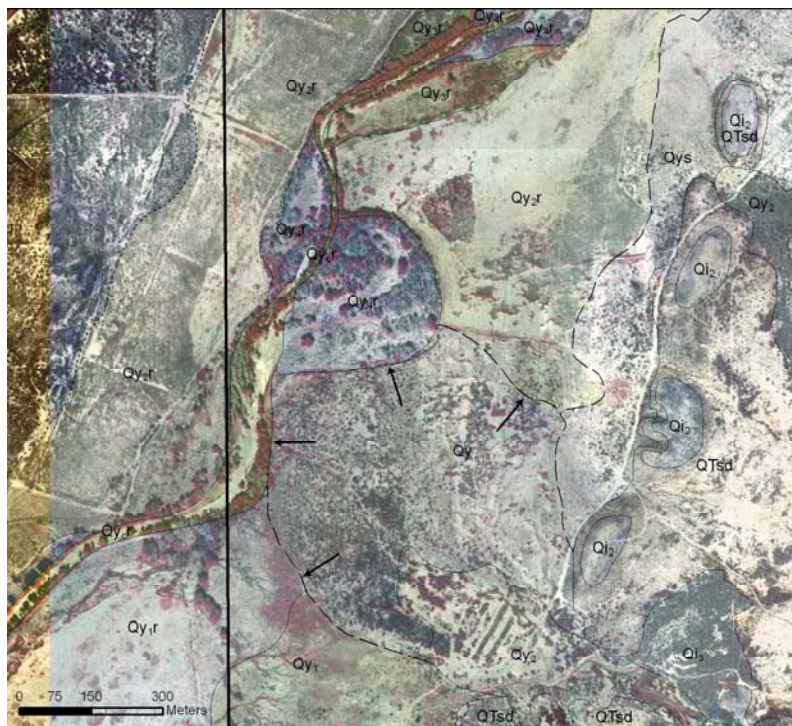


Figure 8. Margins of a large tributary fan (Qy) and Holocene floodplain alluvium. Boundaries between Qy and Qyr and Qy3r are distinct and shown with solid lines. Boundaries between Qy fan and Qy1r and Qy2r are gradual, and thus dashed lines are shown on the map.

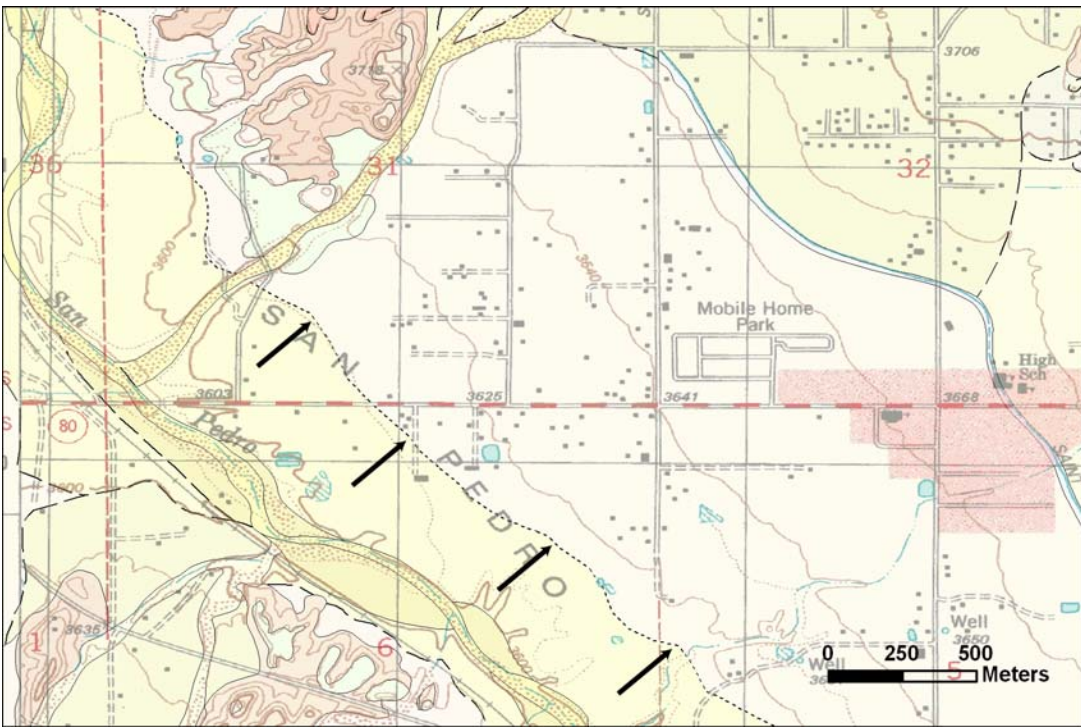
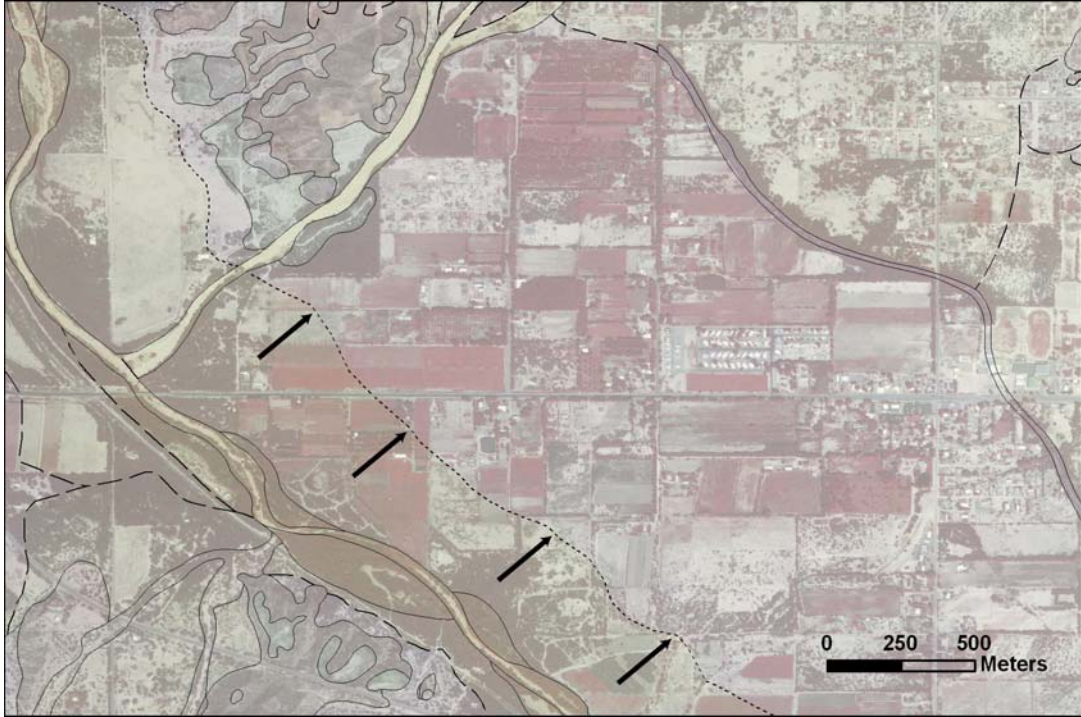


Figure 9. Near populated areas such as Saint David the terrain is very low-relief and heavily disturbed. Dotted line contacts (highlighted by arrows) are used where geomorphic contacts are obscured by anthropogenic activity.

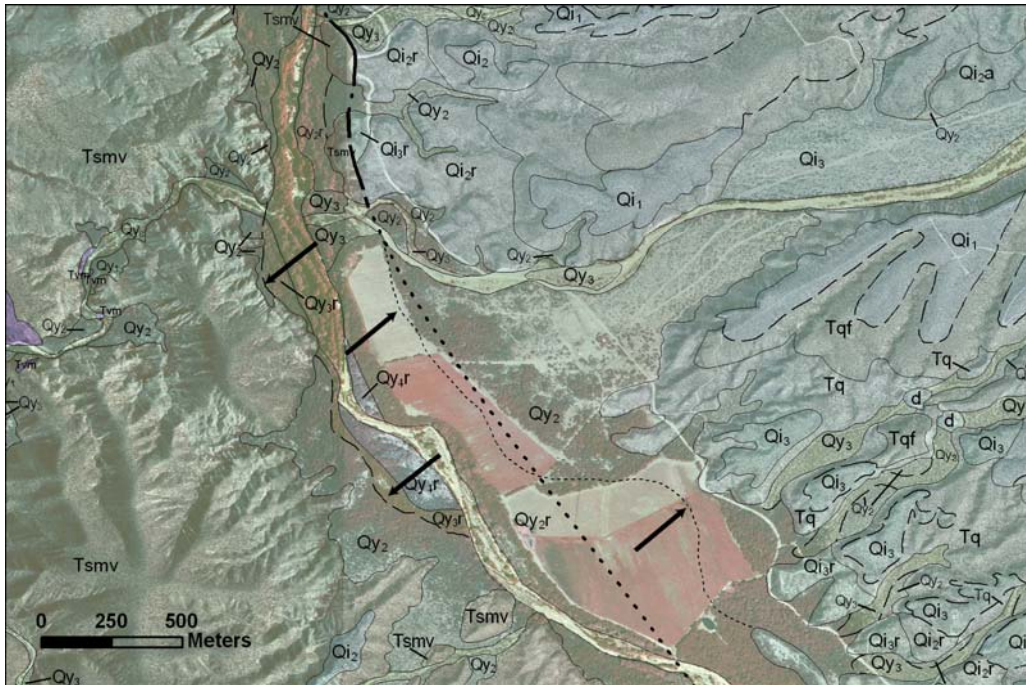


Figure 10. An example of river alluvium adjacent to relatively short fans on one bank (dashed line) and low-relief, presently plowed, distal tributary sediments on the other (dotted line). The heavy dotted line is a concealed fault.



Figure 11. Ground photo (H390-c) taken on east side of San Pedro River looking west as shown in Figure 10. A mix of distal tributary and San Pedro River sediments is currently plowed, obscuring the precise location of the boundary between both units.

and geomorphic criteria outlined previously. Soil survey maps are quite useful in delineating Holocene river alluvium in areas that have been disturbed by anthropogenic activity, however. In addition, soils data and interpretation by NRCS staff provide excellent support for the differentiation of Holocene and Pleistocene deposits (Table 2). Soil survey maps covering the lower San Pedro River are in review (W. Svetlik, oral communication, 2008) and were not available during the course of our mapping.

Extent of Holocene River Floodplain Alluvium. We depict all of the various Holocene river deposits except the active channel with the same map color (dark green) to show the extent of Holocene river alluvium on the strip maps (Map Sheets 1 – 6). Active channels of the San Pedro, Babocomari and Aravaipa streams (Qy_{c,r}) are delineated based on 2005 and 2007 orthophotos. Various surficial and bedrock geologic units that bound Holocene river floodplain alluvium are also depicted in the strip maps.

The lateral extent of Holocene floodplain alluvium varies dramatically along the San Pedro and Babocomari Rivers and Aravaipa Creek (see Map Sheets). In reaches where the streams have cut through bedrock, such as the lower reach of the Babocomari River; along the San Pedro River in northern part of the Lewis Springs quadrangle, several places in the Fairbank quadrangle, and through the Narrows in the Wildhorse Mountain quadrangle; and in Aravaipa Canyon (Figure 12), the lateral boundaries of Holocene floodplain alluvium are sharply defined and the total width of floodplain alluvium is a few hundred feet or less. More commonly, where the river is incised into the basin-fill deposits of the St. David Formation (Lindsay et al., 1990) or the Quiburis Formation (Dickinson, 2003), the width of the Holocene floodplain varies from 1,000 to 3,000 feet. The width of the Holocene river floodplain is less where large tributaries join the San Pedro River, as the alluvial fans deposited by tributaries restrict the lateral extent of deposition by the river. In areas where large, low-gradient tributaries join the mainstem drainages, it can be very difficult to place the contact between Holocene river alluvium and tributary alluvium (Figures 8 and 9).

Although many deposits flanking Holocene river alluvium are also Holocene in age, only several tributary units typically convey surface or near surface flow to the river channel. Qy_c deposits (modern stream channel deposits) occupy the lowest elevation within the piedmont, receive runoff from adjacent surfaces during storms, and convey flow down gradient to the valley axis when infiltration capacity is exceeded. Qy₃ deposits (latest Holocene alluvium) include secondary tributary channels feeding into Qy_c deposits or slightly elevated terraces along piedmont channels. These surfaces are the first to become inundated during higher flow events when channel capacity is exceeded, thereby contributing to the transport of runoff precipitation to the valley axis. Qy_{af} deposits (late Holocene alluvium, active fan deposits) represent the active distributary portion of late Holocene fans. These deposits are typically found where an otherwise confined Qy_c or Qy₃ channel becomes unconfined and surface flow spreads out, dropping transported sediment. Surface flow in piedmont channels often infiltrates into the subsurface of Qy_{af} deposits due to the transition to unconfined flow and the coarse, porous nature of these deposits. Older Holocene units (Qy₂ and Qy₁ deposits for example) occupy higher positions within the landscape and typically do not transmit surface flow under normal conditions. Although precipitation falls throughout the entire piedmont Qy_c, Qy₃, and Qy_{af} deposits represent the active portion of the tributary fan system.

Geologic Map Versions. The AZGS will release a new version of each previously released geologic map (v. 2.0) that is consistent with the delineation of Holocene alluvium depicted in this report. We have made some fairly substantial modifications to the existing geologic maps along the San Pedro River from just north of Benson to the international border and along the Babocomari River. We will release new geologic map versions after final review of our mapping of Holocene river alluvium by ADWR staff and completion of map cartography.

Table 2. Selected soil parameters and age estimates for soils in the southern San Pedro Valley. Age estimates are primarily from P. Camp of the NRCS (written comm., 2003). We have added interpretations of the fluvial source, i.e., river, tributaries, or a mix, based on the NRCS landforms associated with the soil units.

soil mapping unit	component soils	soil class	surface color (YR)	max reddening (YR)	B horizon	landforms	NRCS age class	fluvial source
2	Anthony	torrifuvent	7.5	7.5-10	no	fans	Holocene	tributaries
2	Maricopa	torrifuvent	7.5	7.5	no	fans	Holocene	tributaries
3	Arizo	torriorthent	10	10-7.5	no	fans and floodplain	Holocene	mix
3	Riverwash					river channel	Holocene	river
5	Baboquivari	haplargid	7.5-10	5-7.5	sandy clay loam argillic	fan terraces and stream terraces	Pleistocene	mix
5	Combate	torrifuvent	7.5	10-7.5	no	granitic fans	Holocene	tributaries
7	Bella	petrocalcicid	7.5-10	5-7.5	cemented petrocalcic	fan terraces	Pleistocene	tributaries
8	Blakeney	petrocalcicid	7.5-10	7.5-10	weak petrocalcic	fan terraces	Pleistocene	tributaries
8	Luckyhills	haplocalcid	10	7.5	calcic loam	fan terraces	Pleistocene	tributaries
15	Borderline	calcigypsids	10-7.5	10-7.5	clay argillic	fan terraces	Pleistocene	tributaries
17	Brookline	torrifuvent	7.5	10-7.5	no	floodplains	Holocene	river
17	Fluvaquents	fluvaquent	10	10	no	floodplains	Holocene	river
17	Riverwash					river channel	Holocene	river
32	Combate	torrifuvent	7.5	10-7.5	no	granitic fans	Holocene	tributaries
35	Contention	gypsitorrerts	7.5-5	7.5-5	clay calcic gypsic	dissected lake beds		hillslopes
35	Crystalgyp	haplogypsids	10	7.5	gypsic	dissected lake beds		hillslopes
35	Monzingo	calcipypsids	7.5	7.5	calcic gypsic	dissected lake beds		hillslopes
35	Redington	torriorthent	7.5	7.5	no	dissected lake beds		hillslopes
36	Contention	gypsitorrerts	7.5-5	7.5-5	clay calcic gypsic	dissected lake beds		hillslopes
36	Ugyp	calcigypsids	7.5	7.5	calcic gypsic	stream terraces / fans	Holocene	mix

soil mapping unit	component soils	soil class	surface color (YR)	max reddening (YR)	B horizon	landforms	NRCS age class	fluvial source
39	Courtland	haplargids	7.5-5	2.5-5	sandy clay loam argillic	fan terraces	Pleistocene	tributaries
39	Diaspar	haplargids	5-7.5	2.5-5	sandy clay loam argillic	fan terraces	Pleistocene	tributaries
40	Courtland	haplargids	7.5-5	2.5-5	sandy clay loam argillic	fan terraces	Pleistocene	tributaries
40	Diaspar	haplargids	5-7.5	2.5-5	sandy clay loam argillic	fan terraces	Pleistocene	tributaries
40	Sasabe	paleargids	7.5-5	2.5-5	clay loam argillic	fan terraces and swales	Pleistocene	tributaries
58	Elgin	paleargids	7.5-10	2.5-5	clay argillic	fan terraces	Pleistocene	tributaries
58	Stronghold	haplocalcids	10-7.5	10-7.5	sandy loam cambic	fan terraces	Pleistocene	tributaries
60	Caralampi	haplargids	7.5-5	2.5-5	clay loam argillic	fan terraces	Pleistocene	tributaries
60	Eloma	haplargids	7.5-5	2.5-5	clay argillic	fan terraces	Pleistocene	tributaries
60	White House	haplargids	2.5-7.5	2.5-5	clay argillic	fan terraces	Pleistocene	tributaries
72	Glendale	torrfluvents	7.5	7.5	no	floodplains and stream terraces	Holocene	mix
76	Graveyard	haplocalcids	7.5	7.5	sandy loam cambic	stream terraces and fan terraces	Pleistocene	mix
76	Sierravista	calciargids	7.5-5	2.5-5	clay loam argillic	fan terraces and stream terraces	Pleistocene	mix
79	Guest	torrfluvents	10-7.5	10-7.5	no	floodplains, stream terraces, fans	Holocene	mix
84	Guest	torrfluvents	10-7.5	10-7.5	no	floodplains, stream terraces, fans	Holocene	mix
84	Riveroad	torrfluvents	7.5-10	7.5-10	no	floodplains and fans	Holocene	mix
85	Hantz	torrfluvents	10-7.5	10-7.5	no	floodplains	Holocene	river

soil mapping unit	component soils	soil class	surface color (YR)	max reddening (YR)	B horizon	landforms	NRCS age class	fluvial source
89	Kaboom	calcigypsid	7.5-10	7.5-10	calcic gypsic	stream terraces, fan terraces and relict basin floor	Pleistocene	<i>mix</i>
89	Reeup	haplogypsid	7.5-10	7.5-10	clay calcic	stream terraces and relict basin floor	Pleistocene	<i>mix?</i>
97	Gulch	calciargid	7.5-5	7.5-5	clay loam argillic	stream terraces, fan terraces, relict basin floors	Pleistocene	<i>mix</i>
97	Libby	paleargid	2.5-5	2.5-5	clay argillic	stream terraces and relict basin floor	Pleistocene	
98	Luckyhills	haplocalcid	10	7.5	calcic loam	fan terraces	Pleistocene	<i>tributaries</i>
99	Luckyhills	haplocalcid	10	7.5	calcic loam	fan terraces	Pleistocene	<i>tributaries</i>
99	McNeal	calciargid	5-7.5	5-7.5	clay loam argillic	fan terraces	Pleistocene	<i>tributaries</i>
104	Major	calcigypsid	7.5-10	7.5-10	calcic gypsic	stream terraces and relict basin floor	Pleistocene	
106	Marsh						Holocene	
113	Buntline	petrocalcic	5-7.5	5-7.5	petrocalcic	fan terraces	Pleistocene	<i>tributaries</i>
113	Libby	paleargid	2.5-5	2.5-5	clay argillic	stream terraces and relict basin floor		
113	Nolam	calciargid	7.5-5	5	clay loam argillic	fan terraces	Pleistocene	<i>tributaries</i>
123	Fluvaquents	fluvaquent	10	10	no	floodplains	Holocene	<i>river</i>
123	Quiburi	torrifuvent	7.5-10	7.5-10	no	floodplains	Holocene	<i>river</i>
123	Riverwash					river channel	Holocene	<i>river</i>
125	Riveroad	torrifuvent	7.5-10	7.5-10	no	floodplains and fans	Holocene	<i>mix</i>
125	Ubik	torrifuvent	10-7.5	10-7.5	no	fans and floodplains		<i>mix</i>
127	Bodecker	torriorthent	7.5	10-7.5	no	floodplains and fans	Holocene	<i>mix</i>
127	Riverwash					river channel	Holocene	<i>river</i>

soil mapping unit	component soils	soil class	surface color (YR)	max reddening (YR)	B horizon	landforms	NRCS age class	<i>fluvial source</i>
129	Sasabe	paleargids	7.5-5	2.5-5	clay loam argillic	fan terraces and swales	Pleistocene	<i>tributaries</i>
136	Mule	haplocalcids	7.5-10	7.5-10	calcic	fan terraces	Pleistocene	<i>tributaries</i>
136	Sutherland	petrocalcids	10-7.5	10-7.5	petrocalcic	fan terraces	Pleistocene	<i>tributaries</i>
139	Tenneco	haplocambids	10-7.5	10-7.5	loam cambic sandy loam	floodplains and fans	Holocene	<i>tributaries</i>
142	Tombstone	haplocalcids	10-7.5	10-7.5	calcic	fan terraces	Pleistocene	<i>tributaries</i>
144	Ubik	torrfluvents	10-7.5	10-7.5	no	fans and floodplains	Holocene	<i>mix</i>
150	Moco	argigypsid	7.5-10	7.5-5	clay loam argillic	basin floors	Pleistocene	
150	Vana	petrocalcids	5-7.5	5-7.5	sandy clay loam argillic over petrocalcic	fan terraces	Pleistocene	<i>tributaries</i>

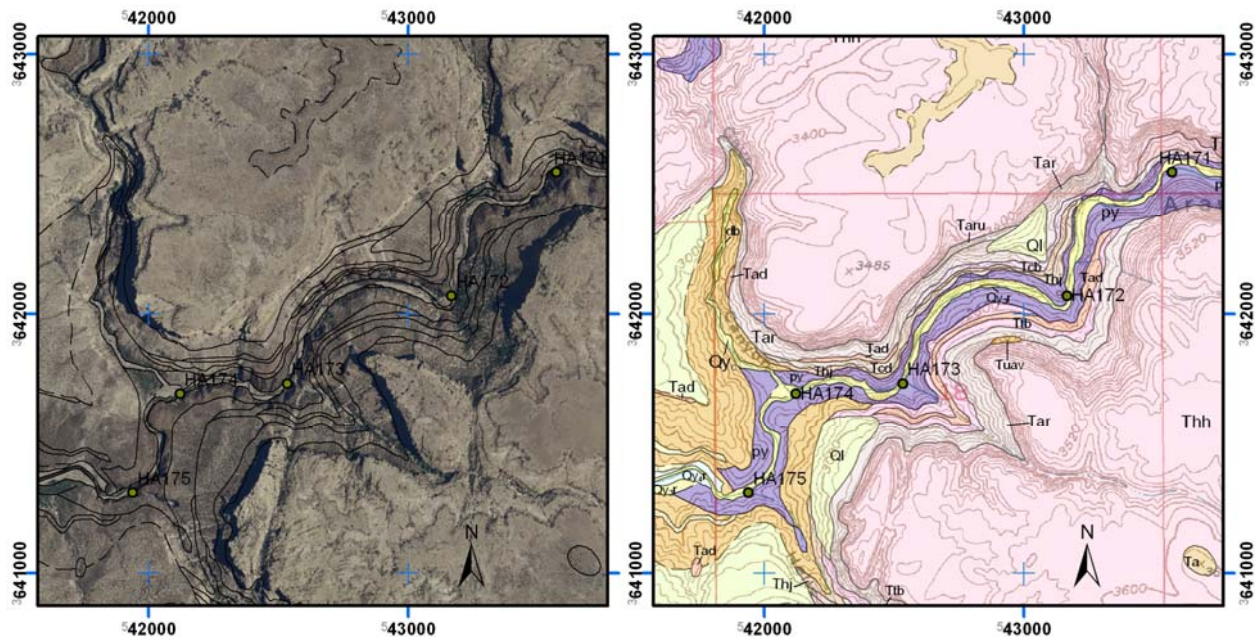


Figure 12. Tight lateral confinement of Aravaipa Creek in Aravaipa Canyon. Aravaipa Creek has incised deeply into resistant bedrock, so the lateral extent of Holocene river alluvium is relatively limited.

San Pedro River Geology and Geomorphology

The San Pedro River is located in southeastern Arizona although its headwaters are about 20 miles south of the U.S./Mexico border in northernmost Sonora. North of the international border, the San Pedro River flows approximately 125 miles to the north-northwest before joining with the Gila River at Winkelman (Figure 1). River altitude ranges from 4,260 ft above sea level (asl) at the U.S./Mexico border to 1,920 ft asl at the Gila confluence. The San Pedro drains an area of approximately 4,720 mi² in Santa Cruz, Cochise, Graham, Pima, and Pinal Counties. Its course traverses deep sedimentary basins flanked by the Huachuca, Mule, Whetstone, Dagoon, Rincon, Winchester, Galiuro, Santa Catalina, and Tortilla Mountains. The San Pedro is fed by numerous tributaries, which in general, drain relatively short and steep catchments oriented more or less perpendicular to the main valley axis (Huckleberry et al, in press). For most of its length the San Pedro flows over sedimentary basin fill deposits, although it is bound by bedrock at the Tombstone Hills at Charleston and near Fairbank, “the Narrows” south of Cascabel, near Redington, and again at Dudleyville (Heindl, 1952). Two major tributaries, Babocomari River and Aravaipa Creek, each have extensive bedrock-lined stretches. Historically the San Pedro has been divided into upper and lower reaches at the Narrows (Heindl, 1952). This division is reflected in the nomenclature for the basin-filling sediments, as deposits south of the Narrows are called the St David Formation while sediments to the north belong to the Quiburis Formation.

Geologic History. The mountains delineating the San Pedro drainage basin generally are north-to northwest-trending fault-block ranges of diverse lithology formed by extensional forces during the Basin and Range disturbance from about 25 to 8 million years ago. As the basin was forming

it was synchronously being filled with sediments eroded from adjacent mountain blocks (Menges and Pearthree, 1989; Huckleberry, 1996). These Tertiary basin filling sediments are coarsest (composed of boulders, large cobbles, and angular fan gravels) near the valley margin and grade to significantly finer sediments (pebbles, sand, silt, clay, and evaporite deposits) near the valley axis (Dickinson, 2003). Initially, these sediments were shed into one or more closed basins in the San Pedro Valley, resulting in a playa to pluvial lake-like environment (analogous to modern Willcox Playa) represented by extensive playa, lacustrine, and marginal playa to distal fan facies presently exposed in the lower San Pedro Valley (Lindsay et al., 1990; Dickinson, 2003). In the late Pliocene to early Pleistocene the San Pedro Valley integrated with the Gila to the north and incision through basin-filling sediments began, resulting in a series of deeply incised drainages, extensive basin fill stratigraphy exposures, and erosional strath terraces often capped by river gravels (Huckleberry et al., in press).

Historical Change. Prior to the late 1800's the San Pedro River was a relatively low-energy, unentrenched fluvial system with extensive marshy reaches, or cienegas (Hereford, 1993). The river floodplain during this time was bound by hills and bluffs composed of distal basin fill sediments shaped by the San Pedro's long-term downcutting and lateral erosion and alluvial fans of various sizes associated with tributary washes. During early historical times the San Pedro was known to be home to beavers, antelope, and numerous species of fish. In some areas a distinct channel was absent and marshy grasslands dominated. Beginning in the 1870s there was modification of the floodplain due to ranching, mining, and the subsequent construction of railroads. Many of the cienegas and beaver ponds were purposely drained to reduce the mosquito population in an attempt to prevent the spread of malaria (Hastings, 1959). By about 1930 most of the San Pedro had been transformed from a low-energy, unentrenched fluvial system with a broad flood plain to a higher energy, in some places deeply incised channel (Cooke and Reeves, 1976; Woods, 1997). Potential causes for entrenchment include the introduction of cattle and subsequent overgrazing, construction of ditches for irrigation along the river, and widespread rangeland fires coinciding with flooding in the late 1800s. Although these factors may have contributed to the widespread arroyo cutting observed along many rivers in the southwest, including the San Pedro, multiple episodes of arroyo cutting and subsequent backfilling occurred prior to the land-use changes associated with the most recent episode of incision and can only be attributed to natural variations in climate, vegetation, and wet-dry cycles (Waters and Haynes, 2001). Although arroyo cutting certainly occurred prior to the historical period without substantial human activity, anthropogenic influence on the landscape may have been a contributing factor in early historical arroyo development (Hastings, 1959; Hereford, 1993; Cooke and Reeves, 1976).

Since historical downcutting, the San Pedro Valley has undergone significant change. Some areas that were once floodplain adjacent to the toes of high-standing basin-fill deposits now consist of a series of inset terraces flanking the entrenched channel. The modern bedload of the San Pedro is coarse compared to the Holocene deposits which it is now incised into, consisting of cobbles, pebbles and coarse sand in many reaches. Deposits exposed in channel walls commonly consist of fine sand, silt, and clay with interspersed pebble to gravel beds (Huckleberry, 1996) as well as organic rich soils associated with cienega deposits (Haynes, 1987; Hereford, 1993). The coarse sediment in the modern channel promotes the formation of point bars and a meandering system which enhances lateral erosion and undercutting of bounding units leading to further widening of the entrenched channel and modern floodplain.

Prior to historical entrenchment of the San Pedro River, vegetation in the valley consisted of tall range and marsh grasses largely void of woody shrubs and mesquite (Hastings, 1959). Since the development of modern San Pedro Valley conditions, mesquite and acacia have become common on the piedmont and dense mesquite bosque is common on pre-entrenchment floodplains (Bahre, 1991; Hastings and Turner, 1965). Identifying the extent of these bosque environments is often useful in delineating boundaries of Holocene river terraces. Within the entrenched channel, riparian vegetation including cottonwood, willow, and sycamore thrive. The location of these stands is useful in identifying the extent of active and flood channel deposits as well as abandoned meanders. In some reaches, particularly just north of Benson and Cascabel, invasive tamarisk fill the channel.

Geomorphology. Prior to widespread arroyo development along the San Pedro, channels, where present, were probably discontinuous and inefficient and hydraulically rough due to ubiquitous tall grasses. Floodwaters were forced to flow more slowly and spread out due to relatively unconfined or weakly incised channel conditions, which promoted infiltration rather than erosion. Since arroyo development the incised channel of the San Pedro River has widened due to bank cutting and collapse, increased surface flow transmitted to the river due to land use and vegetation change, headcutting of disturbed areas, and catastrophic flooding (Huckleberry et al, in press). The historical arroyos were relatively narrow, deep, and vegetation free. This channel geometry acted as a very efficient watercourse for rapid, intense flood discharge (Cooke and Reeves, 1976). The intensity of flows during flood events has the potential to be extremely erosive. The flood of record for the San Pedro occurred in September of 1926 and resulted in substantial bank erosion and channel widening (Huckleberry, 1996).

During low-flow conditions certain reaches of the main channel may be braided and branching, but can transition to a meandering system under higher flow conditions. For much of its reach, the San Pedro can be considered a compound channel. The main channel tends to change position through time due to meander migration and braided channel shifts. The establishment of riparian vegetation flanking the San Pedro River has, in some areas, guarded channel walls and near-channel deposits against erosion. Tree roots can bind soil particles and help stabilize banks. Grasses have a dense fibrous root structure and create surface roughness which helps dissipate flood energy, reduce scour, and encourage channel aggradation. The combination of multiple types of vegetation can armor banks against lateral migration of floodwaters and establish long term stability relative to unvegetated channel walls (Huckleberry et al., in press). Of course this stability has its limits as evidenced by flood damage including large scale uprooting of mature cottonwoods, extensive bank erosion, and numerous debris flows throughout Aravaipa Canyon following several days of heavy rain in the summer of 2006.

Modern channel conditions. The modern floodplain is composed of an incised channel with numerous secondary flood channels and interspersed gravelly bars and low terraces, and typically is hundreds of feet wide (Figure 13). Abandoned meanders and oxbow lakes can be found just south of the bridge crossing the San Pedro on State Route 90. Dense stands of riparian vegetation mark areas along the river where surface or near-surface flow can be found consistently. In these areas it may be possible to observe dry surface conditions during the day and wetter conditions overnight due to the phreatophytic nature of the local vegetation. Sections of the river with shallow bedrock often exhibit at least near-surface water throughout much of



Figure 13. Sandy deposits of the active channel of the San Pedro River (Qycr), deeply incised into late Holocene deposits (Qy2r) that form the high bank on the right side of the photo.

the year simply due to the less permeable nature of bedrock relative to channel sediments. Along the rest of the river as well as on pre-entrenchment floodplain, mesquite, acacia, and tamarisk dominate, sometimes thriving in the channel itself.

Sediments within the active San Pedro channel are generally coarser than the pre-entrenchment alluvium exposed in channel walls. This phenomenon is particularly evident just downstream from steep tributary drainages. Most of these tributaries are dry, sandy washes, although a few major tributaries exhibit occasional flow over at least part of their reaches. Flood flows in these drainages result in the introduction of large pulses of coarse gravelly sediment into the San Pedro channel following precipitation events.

The overall width of the San Pedro active and modern floodplain has been relatively stable since the 1950s (Hereford, 1993). The establishment of riparian and xeric vegetation along and in some places within the channel apparently has slowed (and in some places halted) channel incision and widening. In bedrock lined reaches the San Pedro's floodplain may be confined to 65 – 130 ft across whereas in unconfined reaches the Holocene floodplain reaches up to 1 mile wide. Distal alluvial fans can temporarily onlap onto (and likely interfinger with in the subsurface) late Holocene floodplain deposits (map unit Qy2r). The modern channel is confined within arroyo walls in most places, although some reaches are certainly less incised than others. For this reason the overall width of Holocene floodplain is much more extensive than the modern floodplain except where confined by bedrock or indurated basin fill deposits.

Babocomari River Geology and Geomorphology

The Babocomari River is a major tributary to the upper San Pedro River that flows from west to east between the Huachuca and Mustang Mountains to join the San Pedro River just south of Fairbank. The mainstem of the Babocomari River begins west of Elgin at an altitude of approximately 4,800 ft asl and flows eastward about 25 miles to join the San Pedro River at an altitude of approximately 3800 ft asl. The Babocomari River drains an area approximately 310 mi², including the northern the Huachuca Mountains (7,700 ft asl), northwestern Canelo Hills (5,900 ft asl), and the southern Mustang Mountains (6,450 ft asl). The upper watershed boundary on the mainstem, west of Elgin, is an accordant ridge of high stand basin fill deposits (4,900 ft asl) between the Mustang Mountains and Canelo Hills.

The Babocomari River straddles two Tertiary basins separated by a subsurface bedrock high between the Mustang and Huachuca Mountains (Richard et al., 2007). The upper, western part of the Babocomari drainage is in the Sonoita Basin and lower, eastern part is in the upper San Pedro Basin. The Babocomari River generally flows on Quaternary deposits over Tertiary basin fill sediments (Tsy) in the upper basin and late Tertiary – early Quaternary St. David Formation deposits (QTsd) in the lower basin. Discontinuous bedrock channel sections with thin transient alluvium are common adjacent to the Mustang Mountains, and other bedrock areas, including a reach approximately 1 mile upstream of the confluence with the San Pedro River. Numerous tributaries feed the Babocomari River. Two major tributaries that join the Babocomari River near the Babocomari Ranch headquarters have larger drainage basins than the mainstem. They are Lyle Canyon originating in the northern Huachuca Mountains, and O'Donnell Canyon originating in Canelo Hills.

Geologic History. The headwaters of the Babocomari River are in the middle of Sonoita Basin, which is perched between several mountain ranges and continued to fill with sediment well into the Pliocene (Menges and McFadden, 1981). These finer-grained basin fill deposits were capped by much coarser alluvial fan complexes that date to approximately 3 to 2 Ma (Menges, 1981). The remnant alluvial surface that caps these deposits is known as the Martinez surface (map unit QTa); it records the highest level of basin filling and stratigraphic units in the basin (Menges and McFadden, 1981). In Sonoita Basin, Tertiary basin fill deposits have been divided into lower and upper units; the lower unit reflects earlier extensional tectonics while the upper unit is concordant with the modern basin geometry (Menges and McFadden, 1981). The modern Sonoita Basin is drained in three directions, Sonoita Creek to the southwest, Cienega Creek to

the north, and the Babocomari River to the east. The drainage divide between Cienega Creek and the Babocomari River is a remnant accordant ridge of the Martinez surface.

The lower Babocomari River flows across the upper San Pedro Basin. As described above, the San Pedro River Valley was originally a closed basin with a playa to pluvial-like environment in the central part of the basin. Incised and well-exposed Pliocene to early Pleistocene basin fill deposits (QTsd) in the upper San Pedro River basin are characterized by finer sediments (pebbles, sand, silt, clay, and evaporite deposits) near the valley axis and coarser sediments (gravels, cobbles and boulders) nearer to the adjacent mountains (Pearthree, 2004; Ferguson et al., 2006; Huckleberry et al., in press). As in Sonoita Basin, Tertiary basin fill deposits are capped by Quaternary alluvium.

Historical Change. The Babocomari River was encompassed within the original boundaries of the San Ignacio del Babocomari Mexican land grant. Today, the Babocomari Ranch encompasses 28,000 acres of this original land grant and includes most of the Babocomari River. The towns of Elgin and Huachuca City are located within the upper and lower Babocomari watershed, respectively. Ranching, residential development and gravel mining are the major land uses along the Babocomari River today.

Archaeological investigations reveal a long record of human occupation along the San Pedro and Babocomari Rivers. Most of the sites are Archaic and indicate short-term, seasonal use prior to approximately 2000 years ago (Onken and Huckell, 1989). Archaic occupation along the Babocomari River appears to have been more common during higher energy stream flow (braided streams), and sparse during quieter, cienega-forming periods. The Babocomari River was a boundary between three cultures during AD 500-1100; Mogollon from the north and east, Hohokam from the west, and Trincheras from the south (Onken and Huckell, 1989). Small, scattered villages existed during this time. Larger villages and new pottery types including Babocomari Polychrome, existed during the Classic Period, beginning AD 1100. The Sobaipuri and Pima groups, along with Spanish, occupied the San Pedro and Babocomari Rivers from the 1600's until abandonment of the area in 1835 due to Apache raids (Onken and Huckell, 1989). By the late 1800s the valley was re-occupied with Anglo military, ranching and mining activities.

Land use changes, drought, and cyclical arroyo cutting and filling have been considered principal factors in the widespread arroyo cutting that occurred in many rivers of the southwest starting in the late 1800s (Waters and Haynes, 2001; Huckleberry et al., in press). The river channel incised into the historical floodplain in the early 1900s (Hereford, 1993). By about 1930 most of the San Pedro and its larger tributaries had been transformed from low-energy, un-entrenched fluvial systems to higher energy, deeply incised channels (Cooke and Reeves, 1976).

Geomorphology. Five to eight river terraces have been documented along the Babocomari River through this and previous geomorphic mapping efforts, reflecting three Pleistocene and two Holocene time periods of river aggradation and downcutting (Vice, 1974; Onken and Huckell, 1989; Pearthree, 2004; Ferguson et al., 2006). This suite of terraces along drainages is similar to many other large drainages southeastern Arizona basins (e.g., Menges, 1981). Prior to historical entrenchment vegetation in the valley consisted of tall sacaton and marsh grasses, and was largely devoid of woody vegetation. The river was a low energy, slow moving stream flowing through rough vegetation and cienegas. Geoarchaeological evidence suggests several cycles of higher energy braided systems and lower energy cienegas in the past few thousand years (Onken and Huckell, 1989). The post-entrenchment channel is also a higher energy system with coarser

channel bed material. The channel is generally single-thread probably due to lateral confinement. Since entrenchment of the Babocomari River, vegetation along the river includes cottonwood and willow, is commonly mesquite and acacia on the piedmont, with areas of dense mesquite bosque or sacaton grass on pre-entrenchment floodplains (Bahre, 1991; Hastings and Turner, 1965).

Modern Channel Conditions. The modern channel is confined 3 to 20 feet below historically-abandoned floodplains. The higher energy, single-thread channel is free of riparian vegetation but adjacent inset terraces (Qy3r) have dense riparian vegetation. The banks of historically abandoned river terraces (Qy2r) are very unstable and subject to lateral erosion during high flows (Figure 14). Surface flow within the main channel is found in or near bedrock areas (Figure 15). Channel alluvium within bedrock areas can be thin and discontinuous to absent; the location and extent of material changes with significant flow events.



Figure 14. An example of high, steep banks formed in late Holocene Qy2r deposits along the Babocomari River.



Figure 15. Resistant bedrock forms the lateral boundaries and part of the floor of this reach of the lower Babocomari River. The concrete platform on the opposite bank was part of an old railroad bridge across the river.



Figure 16. Uncinised Babocomari River above the dam at Babocomari Ranch headquarters. View is downstream.

Channel incision is absent at the Babocomari Ranch headquarters where a dam was built as part of watershed restoration efforts begun when the Brophy family purchased the ranch in 1935 (Figure 16). From the ranch headquarters upstream to the confluence with O'Donnell Canyon the floodplain is generally not incised. Vegetation consists of riparian trees along the main channel and marshy, densely vegetated grassy areas across the Holocene alluvium. Above O'Donnell Canyon the influence of the dam diminishes and the channel once again becomes entrenched 3 to 10 feet. Vegetation upstream of O'Donnell Canyon is almost entirely grasses with a few trees in the entrenched channel. Upstream of Elgin floodplain vegetation is entirely composed of grasses.

Aravaipa Creek Geology and Geomorphology

Aravaipa Creek flows north to northwestward from its headwaters approximately 30 miles northwest of Willcox, to its confluence with the San Pedro River between Mammoth and Dudleyville. Aravaipa Creek bears to the north-northwest approximately 25 miles before turning west, passing through the northern tip of the Galiuro Mountains, and joining the San Pedro River another 23 miles downstream. Elevation along Aravaipa Creek ranges from 4463 ft asl at the drainage divide separating Aravaipa from northern Sulphur Springs Valley to 2155 ft asl at the San Pedro confluence. Much like the San Pedro River, Aravaipa Creek passes through a deep sedimentary basin (Aravaipa Valley), where the watershed is bound by the Galiuro Mountains and Black Hills to the west and Pinaleño and Santa Teresa Mountains to the east. Aravaipa Creek has cut dramatically through the Galiuros by way of Aravaipa Canyon. The modern channel flows over sedimentary basin fill deposits of varying levels of induration. Throughout Aravaipa Canyon the channel is largely bound by bedrock with limited sandy to cobbly flood deposits stabilized by dense riparian vegetation (Figure 17). Where bedrock-bound, Aravaipa Creek exhibits perennial flow. Tributaries to Aravaipa Creek are generally dry at the surface much of the year although a few large tributaries are partially spring-fed and may exhibit surface flow more frequently.

Geologic History. Similar to the development of the San Pedro Valley, Aravaipa Creek occupies the axis of an extensional basin formed during the Basin and Range disturbance from about 13 to 5 million years ago. The mode of formation for the Aravaipa Valley is comparable to that of the San Pedro, although the overall width of the basin is narrower. Although no silty playa deposits are exposed in the axial Aravaipa Valley, the overall distribution of Tertiary basin filling sediments is similar to that of the Saint David and Quiburis Formations exposed along the San Pedro (i.e. coarsest near valley margins (cobbles to boulders) and finer (clay, silt, sand and fine gravel) at the valley axis).

Historical Change. Upper Aravaipa Creek was surveyed as early as 1875 and described as a low energy, relatively unincised creek. Several wagon roads existed during this time, some crossing Aravaipa Creek multiple times; one was significant enough to be called the "Globe to Willcox Road". By about 1914 areas south of where the creek was noted years prior were incised by up to 6 feet. The line of entrenchment precisely followed that of the historic wagon trail (Cooke and Reeves, 1976). It is possible the incision along Aravaipa Creek was inevitable based on changing climate and vegetation patterns even without disturbance by man, but the wagon trail likely served as an initiation point for erosion.

Since the initial entrenchment of Aravaipa Creek, headward and lateral bank erosion has progressed resulting in the development of a large arroyo system sometimes reaching up to 1000



Figure 17. Aravaipa Creek in Aravaipa Canyon, with a low Holocene terrace on the far left, the low-flow channel in the left, the flood channel across the bottom of the photo, eroded, indurated basin deposits on the right and in the middle distance, and bedrock cliffs below the skyline.



Figure 18. Recent headward erosion and arroyo cutting has undermined a fence across upper Aravaipa Creek.

ft wide. This erosion is probably on-going, as evidenced by large (60 ft wide) sections of modern fence systems suspended over 10 ft above floors of steep-walled arroyos (Figure 18). Just downstream from the drainage divide the continuity of the main channel has been interrupted by man-made earthen and concrete dams, resulting in aggradation of sediment and loss of a defined channel. This occurs in several places upstream of where the Black Canyon drainage enters the valley axis. Although Aravaipa Creek has undergone incision and arroyo cutting much like the San Pedro River and numerous other drainages in the southwestern US, the level of overall incision is markedly less than that found along portions of the San Pedro River. Channel walls outside Aravaipa Canyon rarely exceed 10-15 ft in height unless the channel is bound by high-standing indurated basin fill deposits.

Vegetation change along Aravaipa Creek is different than that observed within the San Pedro Valley. Thriving riparian vegetation within Aravaipa Canyon has been documented as far back as 1867. Density of riparian vegetation including cottonwood, Arizona ash, and sycamore has increased since the earliest historical records (Webb et al, 2007). Upstream of the canyon mesquite bosque and acacia are common on pre-entrenchment floodplain deposits similar to analogous terraces along the San Pedro River and are useful in delineating the extent of pre-entrenchment floodplain deposits.

Geomorphology. The geomorphic setting of Aravaipa Creek in Aravaipa Valley is very similar to that of the San Pedro. The modern channel is incised into Holocene age floodplain deposits which are in turn inset into relatively high standing hills and bluffs composed of basin fill sediments. Although the geologic setting and bounding units are similar between the two drainages Aravaipa Creek is significantly less incised into adjacent Holocene floodplain deposits than the San Pedro. Additionally, tributary drainages feeding into Aravaipa Creek appear to have a much steeper gradient and are choked with coarse sediment. These short, steep drainages often spill out as coarse fan deposits onto pre-entrenchment floodplain deposits or, in some cases, reach the modern channel.

The steep nature of the majority of tributaries joining with Aravaipa Creek indicates sediment supply exceeds transport capacity within the upper drainage. Much like the San Pedro, the active thread of Aravaipa Creek occupies only a small portion of the modern incised channel. Intense precipitation events enable the channel to shift significantly within the unvegetated channel, sometimes resulting in further widening by lateral bank erosion. Although these periods of flow are intense, they are also generally short-lived and do not result in significant sediment transport relative to the amount stored in tributary drainages. The relative excess of sediment stored in tributary drainages could also be an indication Aravaipa Creek is not yet as mature a drainage system as the San Pedro (i.e. sediment transport out of the basin did not begin as early as the San Pedro's integration with the Gila River).

In the modern channel environment, surface flow emerges near the upstream end of Aravaipa Canyon, probably due to shallow, relatively impermeable indurated basin fill sediments or bedrock. Within the walls of Aravaipa Canyon, bedrock lined Aravaipa Creek is a gently flowing stream, yet has the potential to transition into an extremely powerful, high velocity torrent following intense precipitation events. Debris flows sourced from tributary canyons and steep canyon walls often deliver massive volumes of sediment to the channel following repeated rainy days and saturated hillslope soil conditions. The most recent flood through Aravaipa Canyon

occurred on July 29, 2006 following several days of intense rainfall. The narrow channel and flood plain confined within relatively impermeable bedrock walls throughout Aravaipa Canyon concentrates flow, thereby increasing stream power dramatically. Banks were violently eroded away, undermining long-lived stands of cottonwood and sycamore. These trees were uprooted and transported downstream in a splintered mass which resulted in many more trees downstream broken or uprooted. Numerous initiation points for tributary debris flows that occurred during this storm are evident on 2007 vintage aerial photos.

Modern channel conditions. The observable thread of the active channel upstream from Black Canyon is, in places, weakly incised and difficult to follow. In several areas the channel has been buried by fine grained sediment sourced from tributary drainages. The filling of upper Aravaipa Creek was likely enhanced by historic dams and drainage diversions observed in the vicinity. The first appearance of a continuous unvegetated channel is actually sourced from Black Canyon (Figure 19). Downstream from this area, the most active part of the Aravaipa Creek channel is typically a relatively narrow thread within a wide (300 ft or more) entrenched, sandy, unvegetated flood channel. With each significant flow event the active thread commonly shifts throughout the flood channel, often undermining adjacent 6- to 10-ft tall banks resulting in bank collapse and channel widening.

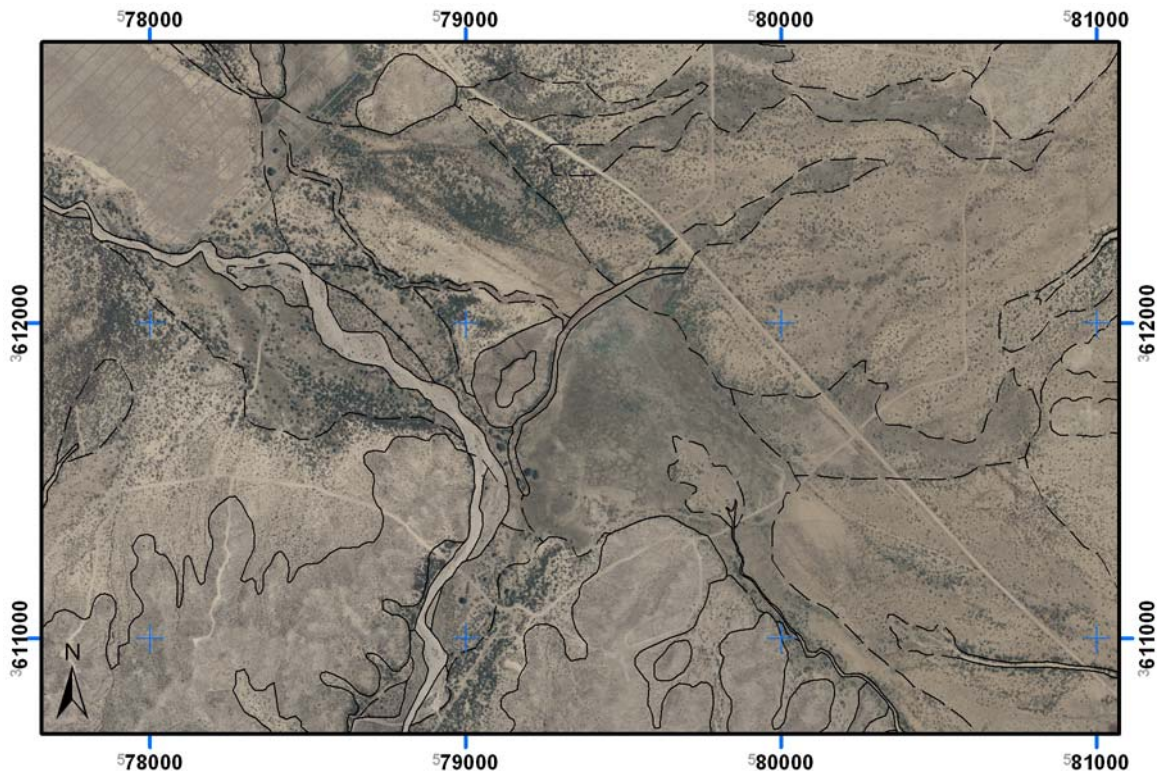


Figure 19. Confluence of Black Canyon and uppermost Aravaipa Creek. Black Canyon enters from the south and is the obvious, light-colored channel. Aravaipa Creek enters from the southeast and has been impounded behind a large earthen dam that was constructed across the flood plain of Aravaipa Creek, resulting in extensive fine-grained deposition. Lately, the dam has been breached in several locations.

Efforts to confine the channel to its present flood channel are evident along several stretches of Aravaipa Creek. Coarse cobbly sediment is often piled into recently eroded sections along outside meander bends of the creek with earth moving equipment. Power line and road repair are commonly required along Aravaipa Creek, especially near the upstream end of Aravaipa Canyon downstream from the emergence zone. Residents living along the creek often experience restricted access to their property and occasionally loss of acreage during moderate to extreme flood events (verbal communication with residents, January 2008). Although some still live within the canyon walls, historic ranch houses and homesteads located further into the canyon were surely inaccessible and prone to flooding during periods of increased channel flow and have been abandoned.

Geoarchaeological Evaluation

Methods. Archaeological data were used to evaluate and refine the age ranges assigned to river terrace deposits on the basis of soil development. Archaeological site locations and descriptive summaries were obtained from Arizona State Museum records using their AZSITE relational database search engine that is accessible through the internet. A polygon depicting the lateral extent of each site falling within the mapped area was plotted on the draft geologic map. Relevant site attributes were then tabulated. These attributes included associated terrace deposits, whether the site was buried or exposed on the modern ground surface, whether or not the artifacts appeared to be reworked by erosion into secondary contexts, USGS quadrangle name, radiocarbon dates, and a brief, general description of the archaeological materials and features found at the site, including temporally sensitive artifact types. Sites spanning multiple deposits were eliminated from this analysis unless the site description specified which deposit was associated with specific archaeological age indicators.

Temporally sensitive archaeological traits are summarized in Table 3. Some archaeological variables are associated with fairly broad temporal parameters, whereas others are quite narrow. For example, plainware pottery dates between 2000 and 250 years before present (BP), whereas Gila polychrome pottery dates from 500–600 BP.

The Paleoindian Clovis Culture, dating to the very latest Pleistocene between 11,500 and 10,900 BP (Waters and Stafford 2007), represents the oldest uncontested human occupation of the New World. Many well-dated Clovis mammoth kill-sites, including the Murray Springs, Lehner, and Naco sites, are located in the San Pedro Valley. Any non-Clovis archaeological material found in a buried context in the San Pedro Valley therefore indicates a Holocene age for the overlying sediment and geomorphic surface, as well as for any inset (i.e., younger) terrace surfaces.

Buried archaeological material (Figure 20) with more precise chronometric bounds can be used to further constrain the age of the overlying terrace surface if the material does not appear to have been reworked. For example, if in situ San Pedro stage (2000–3000 BP) material is contained within a terrace fill, the earlier end of the associated range (i.e., 3000 BP) provides a

maximum age for the overlying terrace deposits. In other words, in this example the overlying terrace deposits would be younger than 3000 BP, and any terrace deposits inset below this terrace would also be inferred to post-date 3000 BP. Similarly, the later end of the associated range (2000 BP) provides a minimum age for the terrace fill deposits underlying the archaeological material, as well as any older deposits or surfaces. Although archaeological material eroded from its original location and deposited in a secondary context also provides a maximum age for overlying deposits, it does *not* provide a minimum age for the underlying deposits because these deposits could be either younger or older than the reworked artifact.

Archaeological surface sites, on the other hand, constrain the *minimum* age of the terrace surface on which they lie because the surface must exist before archaeological material can accumulate. The younger limit of the age range associated with the oldest age indicator found on a surface site generally provides the best minimum age estimate. For example, a type of Hohokam pottery known as Rillito red-on-brown was made from 1000–1150 BP. The presence of a sherd of this pottery type on a geomorphic surface indicates that the surface and the deposits immediately underlying it must be older than 1000 BP.

If surface artifacts are determined to be reworked from archaeological deposits originating on topographically higher geomorphic surface, the artifacts merely constitute one type of clast comprising the deposits capping a younger terrace. Although the older bound of the age range associated with such artifacts provides a maximum age for the reworked sediment, it does not provide any useful age constraints for the underlying terrace, which could be either older *or* younger than the artifact.

Like most dating methods the use of archaeological material for constraining geomorphic surface ages requires certain assumptions. One must assume that the age ranges associated with the various archaeological phenomena are accurate. Also, one must assume that the archaeologist recording the site accurately identified these phenomena. Further, it must be assumed that artifacts were not “curated”, meaning that their prehistoric owners didn’t salvage them from old archaeological sites or, alternatively, reuse or keep or keep an artifact as an heirloom for so long a time that the context that the artifact was finally abandoned in does not temporally reflect the period in which that style was made (Thomas 1979:459). In addition, the geomorphic surface associated with the archaeological material must be correctly mapped, as must be the location of the archaeological site. And finally, when age constraints are derived from archaeological radiocarbon dates, it is assumed that the date reflects the age of the stratigraphic context in which it was found. Charcoal eroded from older deposits and prehistoric burning of “old wood” for fuel (Schiffer 1986) can violate this assumption.

Results

In this section we summarize the archaeological age constraints for various Holocene river floodplain deposits mapped along the San Pedro River and its principal tributaries.

Qy4r. No archaeological sites have been recorded on the Qy4r surface. This is not surprising given that this surface is currently active, undergoing inundation during moderate to high stream-flow events.

Qy3r. Arizona State Museum records initially suggested that nine archaeological surface sites were recorded on Qy3r terraces (Table 5). Five of these sites are historical period sites, consistent with floodplain incision between 1890 and 1930, as proposed by Hereford (1993), and with the historical age assigned to Qy3r.

The other four surface sites initially recorded on this surface contain Hohokam artifacts, suggesting that (1) the Qy3r surface is older than 500 BP, (2) the sites consist of reworked artifacts, (3) the surfaces underlying the sites were incorrectly mapped, or (4) the sites were incorrectly plotted on topographic quadrangles by the archaeologists who recorded them. Several of these sites contain features such as house pits or rock piles suggesting that the archaeological material is not in a secondary context. Field-checking of one of the sites (EE:8:104) determined that the site had been misplotted and actually was located on an adjacent Qy2r surface. Notes describing the location of the three other sites strongly suggest that they are actually situated on Qy2r surfaces and they were interpreted as such in this analysis. Unfortunately, time constraints prevented us from field checking the locations of these sites. All four of these sites, however, were recorded prior to the wide availability of inexpensive and accurate GPS receivers. Prior to 2000, the highest quality signal was reserved for military use, whereas the signal available for civilian use was intentionally degraded, with precision of only about 100 meters.

Qy2r. Seventeen buried and 31 surface archaeological sites containing chronometric information are associated with Qy2r (Tables 4 and 5). The buried sites are all prehistoric, consisting mostly of Archaic (pre-Hohokam) sites dating to the 2000–3000 BP San Pedro stage of the Archaic period and confirming a late Holocene age for Qy2r deposits. Seven of the surface sites contain only historic components, but the others all have Hohokam components post-dating 2000 BP. Nine of the buried sites are dated by radiocarbon. The eleven radiocarbon dates on archaeological features (hearths and roasting pits) found buried 1.4–3.4 m in the Qy2r fill indicate that deposition of the Qy2r fill was underway by roughly 3500 BP, and thus that the channel entrenchment resulting in the formation of the Qy1r terrace occurred before that time. These radiocarbon dates indicate that Qy2r deposition ended sometime after 2000 BP, and temporally diagnostic artifacts and characteristics associated with Qy2r Hohokam surface sites indicate that deposition of Qy2r fill probably ended by around 1000 BP. The presence of Rillito red-on-brown (1000-1150 BP) pottery at two surface sites supports this inference, corroborated by the presence of red wares (800-1500 BP), black-on-white wares (800-950 BP), Rincon red-on-brown (800-1000 BP), Dragoon red-on-brown (850-1200 BP), and/or Dragoon brown-on-buff (850-1250 BP) at seven other surface sites. Only one Hohokam site on Qy2r appears to have

been buried. (EE:7:22 [ASM]) by a thin (20 cm) veneer of floodplain alluvium presumably deposited by a large flood, although a handful of others not considered here were buried under tributary fan deposits. In sum, consideration of all of the archaeological evidence available suggests that most Qy2r deposition occurred between approximately 3500 and 1000 BP, although locally it may include younger deposits.

Hereford (1993:6) believed that the Qy2r fill (which he calls the “pre-entrenchment alluvium”) correlates Haynes’ (1987) Escapule Ranch Formation. Haynes defined the Escapule Ranch Formation in Curry Draw, but Hereford has traced it to the inner valley of the San Pedro River near Lewis Springs, and he thought that the McCool Ranch and Hargis Ranch Members of the formation are expressed as two terraces in the pre-entrenchment alluvium near Hereford. AZGS mapping in the Hereford area suggests that he might be implying that the Qy1r terrace is composed of Hargis alluvium. Haynes (2009:23) dated Hargis alluvium deposition to between about 4000 and 2800 BP. At Curry Draw, he described Hargis alluvium as consisting of “at least 5 m of interbedded medium to coarse arkosic sands, sandy muds, and sandy fine to medium pebble gravels” (Haynes 2007:51).

Hereford (1993:6) stated that the McCool Ranch member represents three periods of deposition, the most recent of which lasted from about 500-100 BP. The archaeological data discussed earlier, however, suggests that Qy2r deposition ended around 1000 BP in most places, consistent with Haynes’ description of the age of McCool alluvium. Haynes (2009:23) found that, after a brief period of degradation, deposition of McCool alluvium began prior 2600 BP and ended about 1000 BP, when a period dominated by floodplain stability and soil formation lasted until the historic arroyo cutting. Haynes describes McCool alluvium at Curry Draw as dominated by finer-grained deposits (muddy sands, sandy muds, and loamy sands) and cienega soils, and thus generally finer textured than Hargis alluvium. Localized arroyo cutting around 1000 BP and subsequent filling until about 500 BP resulted in localized deposition of the Bakarich Ranch alluvium (Haynes 2007:53).

Qy1r. Although several archaeological sites are located on Qy1r surfaces, all of these sites are surface sites. Lacking evidence of buried sites, the late to early Holocene age proposed for Qy1r on the basis of soil development cannot be either confirmed or refuted. The age constraints for Qy2r deposits established using archaeological data, however, do suggest that Qy1r deposits are likely middle Holocene or older. Furthermore, it is plausible that the Qy1r fill is composed of alluvium correlative with one or both of two early Holocene cut and fill deposits documented by Haynes (2007; n.d.) at Curry Draw. Haynes (2009:15) states that the end of the Pleistocene was “marked by the desiccation and erosion of the Coro marl in tributary streams and entrenchment of the San Pedro River.” The Donnet silt, dated between about 9600 and 8000 BP by 20 radiocarbon dates, is composed primarily of wind- and slope-wash-reworked Coro marl (Haynes 2007:48), but Haynes (2009:20) has only observed it in tributary drainages and believes its apparent absence along the San Pedro River is probably because it was completely eroded away during subsequent degradational episodes. Alternatively, it is possible that the Qy1r fill is

composed of the equivalent of Haynes' (2009:22) middle Holocene Weik alluvium, described in Curry Draw as a gray unit consisting predominantly of reworked Donnet silt and Coro marl. Deposition of Weik alluvium began around 6400 BP, following a long period of erosion from about 8000 to 6500 BP, and ended around 3800 BP when there was a period of brief, localized erosion.

Table 3. Temporally sensitive archaeological artifacts and site characteristics.

Description	Age range (yrs B.P.)	Reference
Cultural Periods		
Hohokam (undifferentiated)	500-2000	Cordell (1997)
Archaic/Cochise Culture (undifferentiated)	2000-10,900	Huckell (1990)
San Pedro phase	2000-3000	Sayles (1983)
Clovis	10,900-11,500	Waters and Stafford (2007)
Features		
Pithouse villages	800-2000	Heckman et al. (2000)
Above-ground masonry/adobe structures	500-800	Heckman et al. (2000)
Rock-piles (for agave cultivation)	pre-700	Clark and Lyons (2003)
Ceramics		
Plain ware (undifferentiated)	250-2000	Heckman et al. (2000)
Red ware (undifferentiated)	800-1500	Heckman et al. (2000)
Red-on-brown (undifferentiated)	650-1350	Heckman et al. (2000)
Dragoon red-on-brown	850-1200	Heckman et al. (2000)
Rillito red-on-brown	1000-1150	Heckman et al. (2000)
Rincon red-on-brown	800-1000	Heckman et al. (2000)
Tanque Verde red-on-brown	650-850	Heckman et al. (2000)
San Carlos red-on-brown	500-750	Clark and Lyons (2003)
Red-on-buff (undifferentiated)	500-1250	Heckman et al. (2000)
Dragoon brown-on-buff	850-1250	Heckman et al. (2000)
San Carlos red-on-brown	500-750	Heckman et al. (2000)
Papago red	100-800	Heckman et al. (2000)
Black-on-white (undifferentiated)	800-950	Heckman et al. (2000)
Polychrome (undifferentiated)	500-950	Heckman et al. (2000)
Gila polychrome	500-600	Heckman et al. (2000)
Corregated wares	650-800	Clark and Lyons (2003)

Table 4. Characteristics of Buried Sites Used to Constrain Terrace Ages

Site	Surface	USGS Quadrangle	No. of C14 Dates	Description
BB:11:5 (ASM)	Qy2r	Redington	-	Buried hearth containing burnt maize exposed in arroyo; presence of maize suggests it postdates 4000 BP
BB:11:24 (ASM)	Qy2r	Soza Canyon	-	Likely Archaic burial; extended inhumation with associated chert biface; skeletal material 1.2 m below surface, 30 cm above bottom of wash in coarse matrix
BB:15:2 (ASM)	Qy2r	Galleta Flat East	-	Probable Archaic site with groundstone and charcoal in cutbank exposure; site record implies buried features at 5 m and 7.5 m below surface
EE:4:1 (ASM)	Qy2r	Saint David	-	Prehistoric burial and pit features with San Pedro stage artifacts; thick organic-rich midden (Huckell 1990:300)
EE:4:20 (ASM)	Qy2r	Land	-	Extensive buried archaeological deposit of probable Archaic age exposed in cutbank wall; 3–4 m below surface, 25–45 cm thick, and 100 m long; consists of fire-affected rock, pit features, and flaked stone.
EE:7:22 (ASM)	Qy2r	Huachuca City	-	Hohokam site with grey midden deposit containing plain ware ceramics and flaked stone buried about 20 cm below surface
EE:7:86 (ASM)	Qy2r	Huachuca City	1	San Pedro stage site with burial, flaked stone, groundstone, San Pedro projectile point, and hearth; charcoal from hearth at 1.86 m below surface radiocarbon dated to 2740 ± 70 BP (Onken and Huckell 1989)
EE:7:108 (ASM)	Qy2r	Huachuca City	1	San Pedro stage site with flaked stone, groundstone, and hearth feature at ca. 1.3–3 m below surface; hearth at 1.4 m depth radiocarbon dated to 2740 ± 110 BP (Onken and Huckell 1989)
Isolated hearth ca. 200 m south of EE:7:108 (ASM)	Qy2r	Huachuca City	1	San Pedro stage hearth 2 m below surface with radiocarbon date on charcoal of 3090 ± 120 BP (Onken and Huckell 1989)
EE:7:109 (ASM)	Qy2r	Huachuca City	-	San Pedro stage site with flaked stone, groundstone, San Pedro projectile point, and hearth feature; site buried ca. 2–3 m below surface (Onken and Huckell 1989)
EE:7:110 (ASM)	Qy2r	Huachuca City	-	San Pedro stage site with flaked stone and hearth feature; materials at ca. 2–3 m below surface (Onken and Huckell 1989)
EE:7:111 (ASM)	Qy2r	Huachuca City	1	San Pedro stage site with flaked stone and hearth feature; materials at ca. 2–3 m below surface; hearth at 3 m depth radiocarbon dated to 2930 ± 160 BP (Onken and Huckell 1989)
Haynes locality 250 m east of EE:8:1	Qy2r	Fairbank	1	Rock-lined hearth approximately 3.5 m below surface; wood charcoal from hearth produced date of 2630 ± 150 BP (A-730) (Huckell 1990; Haynes 1966)
EE:8:5 (ASM)	Qy2r	Fairbank	2	San Pedro stage site with San Pedro projectile points, flaked stone, ground stone, fire-cracked rock, and dispersed charcoal; mostly 1–2 m below surface; maize cupules from each locus dated to 2735 ± 75 BP (AA-4810) and 2675 ± 80 BP (AA-4811) (Huckell 1990)
EE:8:7 (ASM)	Qy2r	Fairbank	1	Buried late Archaic site (AZ EE:8:7) with diagnostic San Pedro stage artifacts exposed in arroyo bank (Cattanach 1966; Huckell 1990:301)
EE:8:11 (ASM)	Qy2r (capped by Qy)	Fairbank	2	25–60 cm thick San Pedro stage cultural deposit about 3 m below surface; two domestic structures, 7 pit features, flaked stone, ground stone, fire-cracked rock, ash, charcoal; maize cupules from two of the pit features dated to 2365 ± 75 BP (AA-4808) and 2565 ± 75 BP (AA-4809) (Huckell 1990)
EE:12:2 (ASM)	Qy2r	Hereford	1	Archaic San Pedro stage site with buried hearth dated at 2850 ± 200 BP (A-68) (Wise and Shutler 1958); date on same material also derived by CO ₂ method yielding 1800 ± 140 BP (Damon and Long 1962: 245)



Figure 20. San Pedro stage rock-lined pit eroding out of Qys tributary fan cut-bank at site EE:8:1 (ASM). This feature is buried about 2.3 meters below the modern ground surface.

Geologic Map Units

The following is a comprehensive list of geologic units shown on the map sheets. *Map unit descriptions are extracted from and are consistent with unit descriptions from the various geologic maps that cover the river corridors. See Figure 1, individual map sheets, citations within this section, and the reference list at the end of this report for original sources of the unit descriptions.* Because the strip maps include approximately a mile of surrounding geology on both sides of the river, many piedmont, basin fill, and bedrock unit descriptions are presented here. In some cases numerous subdivisions exist for a particular unit resulting in several separate but similar units and associated descriptions. An effort has been made to standardize unit terminology across quadrangle boundaries. However, in situations where non-AZGS maps were incorporated, unit names and descriptions were not changed, thus some redundant naming exists.

Surficial geological units

Other units

- d - Disturbed ground - Heavily disturbed ground due to agriculture, extensive excavation, or construction of earth dams.
- d - Plowed areas – (hatched symbol on maps) historically or actively plowed fields, irrigated pastures, and other lightly disturbed ground.
- Qtc - Quaternary hillslope talus and colluvium - Thin, steeply to moderately sloping, weakly bedded hillslope deposits mantling the middle and lower slopes of bedrock hills. Deposits are locally derived and very poorly sorted, consisting of angular to subangular basalt cobbles and boulders with a matrix of sand, silt and clay. Older hillslope deposits have darkly varnished cobble and boulder mantles and relatively clay-rich soils.

San Pedro and Babocomari River and Aravaipa Creek alluvium

Holocene Deposits

Qycr - Active river channel deposits - Deposits are dominantly unconsolidated, very poorly sorted sandy to cobbly beds exhibiting bar and swale microtopography but can range from fine silty beds to coarse gravelly bars in meandering reaches based on position within the channel. Clasts are typically well-rounded but may be angular to sub angular. Qycr deposits are typically unvegetated to lightly vegetated and exhibit no soil development. Qycr deposits are entrenched from 30 cm to 10 meters or more below adjacent early historical floodplain deposits depending on location, geomorphic relationship, and local channel conditions. Although much of the San Pedro, Aravaipa, and Babocomari Rivers were perennial streams historically, some sections are dry or marshy at the surface during much of the year. These

deposits are the first to become submerged during moderate to extreme flow events and can be subject to deep, high velocity flow and lateral bank erosion. In some areas of the Babocomari River channel deposits are very thin to discontinuous exposing underlying bedrock. Extent of channel deposit and exposed bedrock varies and shifts with significant flooding.

Qy4r - Flood channel and low terrace deposits - Deposits are found adjacent to active channels in the form of lightly vegetated in-channel bars, small planar fluvial terraces within 30 cm of river elevation, and recent erosional meanders outside the presently active channel. Terrace deposits are inset into older river alluvium and are generally narrow, rarely more than 100 meters across. Qy4r deposits are composed of poorly sorted unconsolidated sediments ranging from fine silts to gravel bars depending on location in the channel at the time of deposition. Pebbles and cobbles are well-rounded to sub-rounded. These surfaces are commonly inundated under moderate to extreme flow events and can be subject to deep, high velocity flow and lateral bank erosion. These deposits do not exhibit soil development but may exhibit a light vegetation cover of small trees, bushes, and grasses.

Qy3r - Historical river terrace deposits - Terrace deposits that occupy elevations from 1 to 2 meters above Qycr or Qy4r deposits and are inset below the pre-incision historical floodplain. These surfaces are generally planar but exhibit bar and swale microtopography. Although no soil development is present, dense grasses and small mesquite trees abound. Sediments composing these deposits are poorly sorted silt, sand, pebbles and cobbles. Pebbles and cobbles are well-rounded to sub-angular. Trough crossbedding, ripple marks, and stacked channel deposits viewable in cross-section indicate deposition in a low to moderate energy braided stream environment. These deposits are prone to flooding during extreme flow events, and undercutting and rapid erosion of Qy3r surfaces is possible during lower flow events.

Qy2r - Latest Holocene to historical river terrace deposits - Deposits associated with the floodplain that existed prior to the early historical entrenchment of the San Pedro and Babocomari Rivers (Hereford, 1993; Huckleberry, 1996; Wood, 1997). Qy2r deposits are associated with broadly planar surfaces that locally retain the shape of historical river meanders. Qy2r surfaces are up to 7 meters above modern Qycr deposits and are the most extensive river terraces in the valley. Qy2r sediments were deposited when the San Pedro and Babocomari Rivers were widespread, shallowly-flowing river systems and are dominated by fine grained floodplain deposits. Dense mesquite bosque and tall grass is typically present on these surfaces except where historic plowing or grazing has taken place. These surfaces appear predominantly fine grained at the surface due in part to the input of organic matter and windblown dust deposition but are composed of interfingering coarse sandy to pebbly braided channel and fine sand to silty river floodplain deposits. Where Qy2r deposits are

moderately to deeply incised they not subject to inundation by river floods, but they may be flood-prone in areas with less channel incision. Qy2r deposits are subject to catastrophic bank failure due to undercutting and lateral erosion during flow events. Distal piedmont fan deposits (Qy2 ,Qyaf, and Qys) onlap onto Qy2r deposits although an interfingering relationship likely exists in the subsurface.

Qy1r - Late to early Holocene river terrace deposits - Deposits associated with slightly higher terraces that represent either higher elements of the early historical floodplain or remnants of older Holocene aggradation periods. These fine-grained terrace deposits commonly have been disturbed by plowing or cattle grazing. When undisturbed, Qy1r deposits are densely vegetated by mature mesquite trees (mesquite bosque) and tall grasses. Soil development is moderate and surface color ranges from 10 to 7.5 YR 4/4. Due to the dense vegetation input of organic matter at the surface is high and often results in a thin (< 10 cm) organic soil horizon. A light dusting (incipient stage I) calcium carbonate accumulation is evident on the undersides of some buried clasts. Qy1r surfaces are up to 7 meters above the active channel in highly incised locales and typically are less than 1.5 m higher than adjacent Qy2r surfaces. Along the Babocomari River Qy1r terraces are found along the valley margins. These terraces typically are covered with fine-grained floodplain deposits, but relict gravel bars and lenses are common.

Pleistocene Deposits

Qi3r - Late Pleistocene river terrace deposits - Terrace deposits are up to 10 to 25 m higher than and up to 500 m outside the margins of the modern San Pedro channel. These deposits consist of well rounded pebbles to cobbles exhibiting stage I+ calcium carbonate accumulation with cross-bedded coarse sandy interbeds. Clast composition is varied and includes rock types not found in the mountains from which modern piedmont material is derived from. Qi3r terrace surfaces are planar, often surrounded by distal piedmont alluvium, and are generally lightly vegetated except for small weeds and grasses. Commonly, Qi3r deposits are inset into adjacent piedmont alluvial deposits but can also be inset into older river gravel terraces. Soil development is weak, possibly due to the porous nature of these deposits.

Qi2r - Middle to late Pleistocene river terrace deposits - Terrace deposits are similar to Qi3r deposits but occupying higher positions in the landscape. Terrace surfaces are slightly to moderately rounded. Clast composition is diverse. Well-rounded pebbles to cobbles with stage I-II calcium carbonate accumulation armor Qi2r surfaces. Vegetation is sparse, consisting of small shrubs and grasses. Soil development is generally weak on Qi2r surfaces, possiblybut soil development is more evident in finer grained sections. Qi2r surfaces are

typically found as high-standing isolated mounds surrounded by distal fan alluvium or as small terraces inset into older fan or basin fill alluvium.

Qi1r - Early to middle Pleistocene river terrace deposits - Deposits are associated with high-standing, well-rounded river gravel terraces. Where Qi1r deposits are extensive, remnant planar caps are preserved near the center of the surface. Qi1r deposits are composed of very well rounded to well rounded pebbles and cobbles from diverse lithologies. Cross-bedded sands with pebbly stringers are interbedded throughout. Near-surface cobbly beds exhibit stage II+ calcium carbonate accumulation. Moderately to strongly calcium carbonate coated clasts or cemented aggregates of clasts mantle the flanks of Qi1r deposits, but clay accumulation is variable, probably due to poor surface preservation. Where surfaces are well-preserved, Qi1r soils are reddened (5-2.5YR), clay argillic horizons, with obvious clay skins and subangular to angular blocky structure. Underlying soil carbonate development is typically stage III-IV, with abundant carbonate through at least 1 m of the soil profile. Sparse small shrubs, weeds, and cacti are present on these surfaces.

Qi1r? - Possible early to middle Pleistocene river terrace deposits - Qi1r? terraces strongly resemble Qi1r river gravel terraces but due to position within the landscape and access restrictions a level of uncertainty remains (Spencer et al., 2009a).

Qir - Pleistocene river deposits, undifferentiated

Qcr - Early Pleistocene river channel alluvium - Unit Qcr is exposed along the hillslopes of the incised river valley beneath identified terraces. Qcr is composed of cobble conglomerate cemented by calcium carbonate. Clasts composition is dominated by volcanic and limestone marl, from the Saint David Formation, lithologies (Shipman et al., 2009).

Piedmont alluvium and surficial deposits

Qyc - Modern stream channel deposits - Active channel deposits composed of very poorly-sorted sand, pebbles, and cobbles with some boulders to moderately-sorted sand and pebbles. Channels are generally incised 1 to 2 m below adjacent Holocene terraces and alluvial fans, but may be incised 10 m or more below adjacent Pleistocene deposits. Channel morphologies generally consist of a single thread high flow channel or multi-threaded low flow channels with gravel bars. Channels are extremely flood prone and are subject to deep, high velocity in moderate to large flow events, and severe lateral bank erosion.

Qy3 - Latest Holocene alluvium - Recently active piedmont alluvium located primarily along active drainages including floodplain, low-lying terrace, and overflow channels. Qy3 deposits are composed of unconsolidated to very weakly consolidated silty to cobbly deposits

and exhibit greater vegetation than Qyc deposits. These deposits generally exhibit bar and swale microtopography and are susceptible to inundation during moderate to extreme flow conditions when channel flow exceeds capacity. Soil development is generally absent or incipient on Qy3 deposits which exhibit pale buff to light brown (10 YR) surface coloration.

Qyaf - Late Holocene alluvium, active fan deposits - Qyaf deposits consist of active alluvial fan deposits in the San Pedro valley. These deposits have distributary drainage patterns and are extremely prone to flooding and channel migration. Sediments are unconsolidated and consist of very poorly sorted sand to cobbles. Vegetation includes small mesquite trees, shrubby acacia, prickly pear, and medium creosote.

Qy2 - Late Holocene alluvium - Young deposits in floodplains, low terraces and small channels that are part of the modern drainage system. Along the larger drainages, unit Qy2 sediment is generally poorly to very poorly sorted silt, sand, pebbles, and small cobbles; floodplain and terrace surfaces typically are mantled with sand and finer sediment. On lower piedmont areas and in smaller tributary washes young deposits consist predominantly of moderately sorted sand and silt, with some pebbles and cobbles in channels. Soils are pale brown in color (10 YR), and soil development is very weak, consisting of slight carbonate accumulation. Channels generally are incised less than 1 m below adjacent terraces, but locally incision may be as much as 2 m. Channel morphologies generally consist of a single-thread high flow channel or multi-threaded low flow channels with gravel bars adjacent to low flow channels. Channels are flood prone and may be subject to deep, high velocity flows in large flow events. Potential lateral bank erosion is severe, and flood flows may significantly change channel morphology and flow paths. Local relief varies from fairly smooth channel bottoms to undulating bar-and-swale topography that is characteristic of coarser deposits. Terraces have planar surfaces, but small channels are common.

Qy1 – Older Holocene alluvium - Qy1 deposits consist of terraces along tributary drainages and broad, low-relief, undulating fan deposits, that exhibit shallow widespread braided drainage patterns, and sit higher in the landscape than younger Holocene alluvium. Portions of these deposits are mantled by coarse to very coarse angular quartz sand and exhibit diverse vegetation patterns dominated by cholla, prickly pear, small (1-1.5 m tall) mesquite, and numerous small shrubs and grasses. Overall relief between broad fan crests and incised drainages on gently rolling Qy1 deposits typically does not exceed 1.5 meters. Numerous shallow braided channels drain widespread portions of Qy1 surfaces. Qy1 deposits exhibit incipient calcium carbonate accumulation (stage I) and soil development characterized by medium brown (10-7.5 YR) coloration where unincised. Deposition of Qy1 sediments in a braided channel aggrading alluvial fan environment has, in places, resulted in shallow burial of adjacent piedmont deposits. This relationship is visible along incised channels where thin Qy1 deposits overly redder, grusy, clay-rich Qi2 or Qi3 deposits.

Qys - Holocene fine-grained deposits - Unconsolidated, very fine to fine grained alluvium located in close proximity to basin fill deposits. These sediments are lighter in color and finer than alluvium derived from further upfan. In general, Qys deposits are loamy silts to fine sands and may contain moderate amounts of gypsum fragments derived from basin fill deposits. Vegetation on Qys deposits consists of small shrubs, grasses, creosote, and acacia.

Qyp - Late Holocene spring deposits (present) - Unit Qyp is related to the only spring feed swamp on the mapped area. Although much of the swamp is drying the landscape is modified by the springs presence. Qyp deposits are composed of clay loam and have a high percentage of expanding clays (smectite). Much of this surface is barren except the portions that are still wet. In the wet portion of the surface cattails and sacaton grasses crowd the landscape. In the dry portion of this surface dissection and incision have begun, with abundant vertical surface cracks developing (Shipman et al., 2009).

Qy - Holocene alluvial deposits, undifferentiated - Unit Qy consists of undivided Holocene deposits in small channels, floodplains, low terraces, and alluvial fans on the upper piedmont where these deposits are not extensive enough to map as individual Qyc, Qy2 or Qy1 deposits at a scale of 1:24,000 (Ferguson et al., 2009).

Qs - Surficial deposits, undivided - Includes fine-grained colluvium and alluvium, talus, and some pediment and terrace gravels (Krieger, 1968b).

Ql - Landslide deposits - Consist largely of Galiuro Volcanics, locally cemented with caliche (Krieger, 1968a).

Qt - Talus - Rock debris consisting of large angular blocks to silt-sized particles, locally cemented with caliche (Krieger, 1968a).

Qp - Pediment gravel veneer - Gravel veneer on pediments and lower terraces (0-25 ft).- Largely subangular pebbles and cobbles of Paleozoic and Pre-cambrian rocks in a generally reddish-brown, fine- to coarse grained matrix. Reddish-brown color less pronounced on younger terraces and generally lacking on higher level (above 4,000 ft), older(?) surfaces where gravels are composed largely of Galiuro Volcanics. Locally includes some pediments and terraces stripped of gravels (Krieger, 1968a).

Qyi - Holocene and Pleistocene alluvium - Mixed fine-grained Holocene (Qy) and Pleistocene (Qi2 or Qi3) alluvium. In some areas, surficial deposits are primarily Holocene, but these deposits are quite thin and some Pleistocene deposits are exposed along channels. In other

areas, surficial deposits are primarily Pleistocene but there Holocene deposits in topographically low areas (Pearthree and Youberg, 2009).

---Break between Holocene (Q_{y_n}) and Pleistocene (Q_{i_n}) piedmont units---

Qi3c - Late Pleistocene alluvium - Unit Qi3c consists of weakly to moderately dissected alluvial fan deposits. Qi3c deposits are composed of clay loam mudstone. Qi3c surfaces mantel Saint David Formation usually as broad distributed fans. Qi3c surfaces are patchy and planar sloping toward the valley that is broadly dissected. Qi3c source primarily Paleozoic limestone outcrops. Qi3c soils are weak to moderately developed, 10 YR 6/4 light brown, stage I to II secondary nodular carbonate present in the profile, with columnar peds. Qi3c has no desert pavement. Qi3c represents a broad alluvial fan deposit across the moderately dissected fan surface. Qi3c is primarily vegetated by creosote and sparse acacia (Shipman et al., 2009).

Qi3a - Late Pleistocene alluvium - Unit Qi3a consists of deposits that fill the valleys incised into the Saint David Formation, Q_o, and Qi₂ alluvial fan complexes. Qi3a deposits are composed of mudstone with some floating cobbles within the mud matrix. These surfaces are flat with punctuated slot incised channels. Qi3a has portion of the surface that are relatively unincised with to up to 3m of incision down tributary toward the San Pedro River. Closer to the river isolate remnants of Qi3a outcrop along the tributary valleys. Soils are weak to moderately developed with of clay loam, small blocky peds, 7.5 YR 5/4, and filament carbonate. Qi3a surface appear as buff in air photos. Qi3a is dominated by sacaton grasses and medium size mesquite trees. Qi3a represents the valley fill that is subsequently incised due to down cutting in the San Pedro River (Shipman et al., 2009).

Qi3 - Late Pleistocene alluvial fan and terrace deposits - Widespread planar orange to reddish relict alluvial fans and terraces mantled by angular to sub-angular pebbles to cobbles. These deposits exhibit moderate calcium carbonate accumulation (stage I-II) and soil development with reddish shallow subsurface coloration (7.5 YR 4/4). This color varies with position in the piedmont due to differences in parent material (mixed granitic, carbonate, and metamorphic clasts on the west side of the river vs. predominantly Galiuro volcanic clasts to the east). Qi3 deposits exhibit medium (1-2 m tall) mesquite, cholla, prickly pear, creosote, acacia, and numerous small grasses and shrubs. Qi3 deposits stand up to 3 meters higher in the landscape than adjacent Q_{y1} and Q_{yc} deposits depending on local incision and position within the piedmont (Cook and Spencer, 2009).

Qi2b - Middle to late Pleistocene alluvial fan and terrace deposits (youngest member) - Qi2b deposits strongly resemble Qi₂ and Qi_{2a} deposits but are inset into both along major

drainages. Surface coloration, vegetation, and soil development are all very similar to those found on Qi2 and Qi2a deposits (Cook and Spencer, 2009).

Qi2a - Middle to late Pleistocene alluvial fan and terrace deposits (younger member) - Qi2a deposits strongly resemble Qi2 deposits but are inset into these deposits along major drainages. Surface coloration, vegetation, and soil development are all very similar to those found on Qi2 deposits (Cook and Spencer, 2009).

Qi2 - Middle to late Pleistocene alluvial fan and terrace deposits - Deposits associated with broad planar alluvial fans and terraces with strongly developed reddish soils that cap Quiburis basin fill deposits and are inset below older, more well-rounded alluvial surfaces. These deposits generally exhibit reddish (5 YR 5/4) soils and moderate calcium carbonate accumulation (stage I-IV). Qi2 deposits are overall planar but can exhibit mild to moderate rounding near incised channels or inset terraces. Vegetation on Qi2 surfaces consists of medium mesquite, prickly pear, cholla, barrel cactus, and numerous small shrubs and short grasses. Where incised, these deposits often exhibit a cap up to 1 meter thick of moderately calcium carbonate cemented clasts. This cap preserves underlying, less-indurated portions of the Qi2 surface as well as any deposits it may overlie. Qi2 terraces deposited onto basin fill deposits may stand as much as 30 meters above active piedmont channels (Cook and Spencer, 2009).

Qi1 - Early to middle Pleistocene alluvial fan and terrace deposits - Qi1 deposits are characterized by high-standing, moderately to well-rounded alluvial deposits exhibiting strong (stage II-III) calcium carbonate accumulation and, where preserved, clay loam argillic soils (5-2.5YR 4/6), with obvious clay skins and subangular blocky structure. Like Qi2 deposits, Qi1 deposits may cap underlying basin fill deposits. Where widespread (greater than 30 meters across), Qi1 deposits retain a remnant, indurated planar cap with moderately to well rounded edges. Narrow (less than 30 meters across) Qi1 terraces and caps are generally well-rounded and do not exhibit a planar remnant. Qi1 terraces are commonly mantled by coarse pebbles to boulders and exhibit vegetation consisting of medium to large mesquite, acacia, saguaro, prickly pear, cholla, barrel cactus, and grasses. Qi1 surfaces around the Mustang Mountains in the Babocomari River drainage are derived from several carbonate bedrock units (Hayes and Raup, 1968). These Qi1 fans have little to no surface reddening and are high, rounded ridges with very coarse deposits due to the proximity of the mountains (Cook and Spencer, 2009).

Qi - Pleistocene alluvial deposits, undifferentiated (Pearthree et al., 2009b)

Qiu - Pleistocene alluvial terrace - undivided - coarse clastic alluvial fan and terrace deposits with slightly to moderately reddened soils (Young et al., 2009)

Qo – Early Pleistocene alluvial fan deposits - Deposits associated with very high relict alluvial surfaces. A remnant planar cap may be present on extensive surfaces such as ancestral planar alluvial fans. Where preserved, soils on Qo surfaces exhibit clay-rich argillic and well developed calcic horizons. Dark red soils (2.5 YR 4/6) are sparsely covered by mild to moderately varnished pebbles to small cobbles. Near surface soil is loamy and overlies much coarser clasts visible on the eroded flanks of Qo surfaces. Vegetation consists of tall saguaro, palo verde, prickly pear, mesquite, and isolated creosote. Remnant argillic horizons exhibit clay faces, blocky ped structures, and are deep red in color. Exposures of the calcium carbonate horizon exhibit stage III to IV accumulation. Qo deposits average 5 meters to as much as 15 meters thick. Aggregate chunks of eroded portions of the carbonate horizon commonly litter the flanks of Qo and underlying deposits. Qo surfaces generally occupy the highest position in the landscape, capping Quiburis basin fill deposits. Thin relict ridge-capping reaches of Qo deposits are commonly encountered where the underlying basin fill deposits are highly eroded and incised. Underlying basin fill deposits stand much higher in the landscape relative to comparable, uncapped deposits (Cook and Spencer, 2009).

QTa - Late Pliocene to early Pleistocene fan gravel - Coarse gravelly deposits that erosionally overlie Quiburis basin-fill conglomeratic facies and form the upper parts of high, very rounded ridges. QTa deposits are composed of very poorly sorted angular to sub angular sand, pebbles, cobbles, and boulders arranged in alternating fine to coarse beds common in alluvial fan deposits. High standing rounded ridges are composed of carbonate-cemented conglomerate cap which armors the underlying, less indurated basin-fill sediment. The flanks of QTa ridges are also armored against erosion due to the mantle of coarse clast cover derived from weathered sections of the cap. Exposures of QTa deposits are generally poor, but they may locally be at least 30-40 meters thick and are commonly the highest standing deposits in the proximal piedmont (Cook and Spencer, 2009).

QTc - Conglomerate (Pliocene to Pleistocene) - Conglomerate is massive to crudely stratified, poorly bedded to massive. Subangular clasts are typically 5-50 cm, and locally up to 1 m. Near north edge of quadrangle, clasts consist dominantly of Johnny Lyon Hills Granodiorite, with less common Pinal Schist and miscellaneous other granitoids and vein quartz. In northeast corner of quadrangle, clasts include probably Scanlon Conglomerate derived from the Pioneer Shale of the Apache Group, which is exposed to the northeast in the Johnny Lyon Hills (Cooper and Silver, 1964). Interpreted as alluvial fan deposits shed into San Pedro River Valley from flanking bedrock hills and mountains (Youberg et al., 2009b).

QTcs - Conglomerate and sandstone (Pliocene to Pleistocene) - Coarse, poorly sorted, tan sandstone, conglomeratic sandstone, and conglomerate. Some sandstone and conglomeratic sandstone are pinkish tan to reddish tan to reddish medium brown. Poorly to moderately defined beds are generally 20 to 100 cm thick. Most clasts are 1-20 cm diameter, locally to

50 cm. Conglomerate clasts are mostly granitic and subangular to subrounded. Conglomeratic sandstone beds commonly contain channels and channel fill pebbles and cobbles that are coarser than host. Typical channel is 1 m wide and 20 cm deep. Some beds have 2-20 mm granules and pebbles in lower 5-10 cm, with crudely graded beds. Locally, near basin axis but adjacent to bedrock outcrops, unit consists of poorly bedded and poorly sorted sandstone with spars 1-10 cm angular granite debris. This unit interfingers with units QTc near its top and Ts near its base (Youberg et al., 2009b).

Tertiary Basin Fill alluvium

QTsd - Pliocene to early Pleistocene Saint David Formation - Relatively thick sequences of red to green siltstone and claystone, white limestone, and buff sandstone. This unit is typically relatively erodible and is poorly exposed on slopes below capping Quaternary gravels. Limestone and sandstone beds are typically more resistant and form ledges. Exposures in the eastern 1/2 of the Lewis Springs quadrangle belong to the middle member of the Saint David formation (Lindsay et al, 1990), which is dominated by fine-grained floodplain deposition associated with a north-flowing axial drainage. Limestone beds may represent local marsh or lacustrine environments. Deposits in the western part of the quadrangle are coarser and probably represent distal fan environments. Local zones of substantial clay and carbonate accumulation near the modern valley axis may represent moderately developed buried soils (Pearthree et al., 2009b).

QTsl - Lacustrine facies of the Saint David Formation (Pleistocene to Pliocene) - Tabular limestone beds are found with interbedded with red and green mudstones. Limestones are composed of structureless chalky micritic calcite. Globular calcium carbonate nodules that are classified as stage III to IV carbonate are found within a muddy matrix on the peripheral facies. Interbedded mudstones vary in color from red to greenish blue. Tuffs with fine to medium grained sandstones are common throughout this formation (Shipman et al., 2009).

QTsc - Pliocene-Pleistocene channel conglomerates - Piedmont channel conglomerates composed of consolidated, matrix supported, moderately to well sorted, subangular to rounded pebble, cobbles and sand. Generally this unit was found within QTsp but at many different elevations. Just east of the town of Saint David this unit is found at the base of QTsp and directly on top and interfingered with unit Tsp. In other areas it is found with in QTsp. And in some places these channel deposits were mapped within Qsf (Youberg and Cook, 2009).

QTbf - Early Pleistocene fine-grained basin-floor alluvium - Unit QTbf consists of very old relict basin floor deposits forming a minimally dissected surface that dips gently to the northeast in the northeastern part of the map area. The QTbf surface is brown in color, with abundant

carbonate litter derived from the underlying petrocalcic horizon. Surface deposits are primarily sand and silt, with little or no gravel. Exposures around the margins of the plateau reveal the existence of a ~1 to 2 m thick carbonate cemented layer that is probably a petrocalcic horizon. Small, uncised swales evidently convey surface runoff across this surface, and deposits ranging in age from Holocene to middle Pleistocene appear to lap onto the QTbf surface from the Whetstone-Mustang piedmont. QTbf deposits in this area sit immediately above basin-fill deposits, probably the middle St. David Formation (Youberg et al., 2009b).

Tsy - Pliocene to middle Miocene deposits - Moderately to strongly consolidated conglomerate and sandstone deposited in basins during and after late Tertiary faulting. Includes lesser amounts of mudstone, siltstone, limestone, and gypsum. These deposits are generally light gray or tan. They commonly form high rounded hills and ridges in modern basins, and locally form prominent bluffs. Deposits of this unit are exposed widely in the dissected basins of southeastern and central Arizona.

Tsp - Playa facies of the Saint David Formation - Gypsum found as tabular layers in some cases below this layer selenite litters the outcrop. Thick tabular gypsiferous layers interbedded with limestones and mudstone (Youberg and Cook, 2009).

Ts - Red sandstone, silty sandstone, and siltstone - Massive to bedded, reddish brown (5YR to 10YR) sandstone, siltstone, and mudstone that forms low-relief outcrops. Outcrops are commonly mantled in dried mud with polygonal fractures that possibly formed by expansion of clay minerals. This unit correlates to the lower Saint David Formation of Gray (1965), and Smith (1994), (Youberg et al., 2009b).

Tsd - St. David Formation, undifferentiated - St. David Formation which includes the lower and middle members (Youberg et al., 2009a).

Tsdl - Lower member of the St. David Formation - Lower St. David Formation consists of red mudstones and fine grained sandstones with nodular and fibrous gypsum located in the mudstones (Youberg et al., 2009a).

Tqc - Late Miocene to Pliocene Quiburis deposits, alluvial fan facies - Gravelly alluvial-fan and braidplain facies. Gray to buff-colored deposits vary from massive, sand-rich beds that predominate in the lower piedmonts to imbricated pebble-cobble-small boulder beds higher on the valley margins. In some areas, Tqc deposits grade into alternating thin unconsolidated beds of gypsum, silt, and very fine sand with occasional pebble stringers (Tqc deposits) along the valley axis. Tqc sediments are encountered throughout the mapped area and are generally well-exposed in deeply incised piedmont channel walls. In these exposures, Tqc deposits are

often observed as capped by relict QTa, Qo, or younger (Qi1 to Qi3) deposits (Dickinson, 2003).

Tqe - Pliocene Quiburis deposits, low energy fluvial deposits - Tqe deposits are located along the axis of the San Pedro Valley and represent a period of sedimentation in a closed basin prior to the initiation of the San Pedro River (Dickinson, 2003). Tqe deposits are composed of alternating thin unconsolidated beds of gypsum, silt, and very fine sand with occasional pebble stringers. The environment of deposition for these deposits was most likely a low energy axial fluvial system with either overbank stillwater or levee zones which allowed standing water to accumulate. The presence of pebbly beds or stringers indicates these deposits are not indicative of a lacustrine environment. Repeated episodes of sedimentation and evaporation of ponded water have resulted in stacked deposits observable within walls of incised drainages near the valley axis. The fine grained character of Tqe deposits becomes gradually coarser upfan. Tqe deposits are light to medium brown in color and are easily erodible unless protected by an indurated capping unit. Uncapped Tqe deposits are commonly observed to form intricately-dissected mounds similar in appearance to those found in badlands landscapes. The flanks of these mounds are often littered with gypsum crystals (Cook and Spencer, 2009).

Tql - Pliocene Quiburis deposits, playa-lacustrine facies - Laminated lacustrine facies includes interbedded mudstone, limestone, gypsum, and diatomite beds of varying thickness, with sparse and thin intercalations of laminated lacustrine sandstone (Dickinson, 2003).

Tqm - Pliocene Quiburis basin fill deposits, prodelta mudstone facies - Massive prodelta mudstone deposited as foredelta facies of "Eskiminzin Delta" (Dickinson, 2003).

Tqs - Pliocene Quiburis basin fill deposits, sandy fan toe facies - Sandy fan-toe, lake-margin, and delta-front sandflat facies (massive to laminated sandstone with minor shale or mudstone interbeds and local thin pebble stringers) intermediate in both grain size and depositional environment between laterally equivalent alluvial-fan/braidplain (Tqc) and lacustrine (Tql & Tqm) facies (Dickinson, 2003).

Tqse - Pliocene Quiburis basin fill deposits, delta front subfacies - Prominent delta-front subfacies (sandstone, locally pebbly, with multiple thin mudstone interbeds) of "Eskiminzin Delta", where the axial fluvial system flowing to the southeast down the Gila segment of the San Pedro trough debouched into the axial lacustrine system of the San Pedro segment of the San Pedro trough near an array of partly buried tiltblocks that expose Galiuro Volcanics near Dudleyville (Dickinson, 2003).

Tqa - Pliocene Quiburis basin fill deposits, distal fan to axial valley deposits - Tqa deposits are located along the axis of the San Pedro Valley and represent a period of sedimentation in a closed basin prior to the initiation of the San Pedro River (Dickinson, 1998, 2003). Tqa deposits are composed of alternating thin unconsolidated beds of silt to very fine sand with sparse pebble stringers. In some areas small gypsum flakes are found on the eroded flanks of Tqa deposits. Fine-grained Tqa deposits grade up-fan into coarser clastic deposits. Tqa deposits are light to medium brown and are easily erodible unless protected by an indurated capping unit. Uncapped Tqa deposits are commonly observed to form intricately-dissected mounds similar in appearance to those found in badlands landscapes. The flanks of each mound often exhibit "elephant skin" textures. Tqa deposits are similar to QTsd deposits mapped south of the Narrows in the Galleta Flat East quadrangle (Youberg et al., 2006) and in quads further south (Spencer et al., 2009a).

Bedrock Units

Tgv - Galiuro Volcanics - Oligocene-Miocene Galiuro Volcanics; lateral equivalent of Cloudburst Formation (Dickinson, 2003).

Tsc - Sandstones and conglomerates - Reddish mudstones and sandstones to tan sandstones and conglomerates found in and along the channel of upper Babocomari River and on adjacent ridge noses in the western part of the basin. Beds are variously tilted. Previously mapped by Hayes and Raup (1868) as older, deformed gravels (Tg). Vice (1974) mapped the reddish mudstones and sandstones as Bisbee group (Kb) and the tan sandstones and conglomerates as Pantano equivalent (Tp). May be correlative to Menges (1981) Canelo Hills Sedimentary Rocks (Tsc).

Tgm - Mafic dikes - Mapped by Hayes and Raup (1968), Mafic dikes within or adjacent to older deformed gravels, Tg.

Tsmv - Conglomerate, San Manuel Formation, volcanoclastic Soza Canyon facies - Clasts are derived primarily from volcanic rocks like those that make up most of the Galiuro mountains as well as locally exposed volcanic rocks beneath the conglomerate in lower Soza Canyon (Dickinson, 1991, Spencer et al., 2009c).

Tsmm - Conglomerate, San Manuel Formation, metamorphiclastic Paige Canyon facies - Clasts are derived primarily from metamorphic tectonites like those that form nearby bedrock in the Little Rincon Mountains (Dickinson, 1991, Spencer et al., 2009c).

Tvm - Mafic volcanics of lower Soza Canyon (Oligo-Miocene) - Dark gray to black, somewhat crystal poor lava-flow breccia and local flow cores. Thin-section examination (very fresh

sample 3-7-07-1 from station JES-07-546) reveals ~10%, >2 mm plagioclase, and ~2-3%, <1 mm pyroxene(?), in black matrix with abundant, very fine acicular plagioclase. The high-relief tabular mineral, with up to second-order blue in polarized light, is inferred to be pyroxene and not hornblende because it is not pleochroic. Volcanics are 98% breccia, but clasts of mafic volcanics are generally rounded as if tumbled in a volcanic flow breccia. Matrix is indurated as if composed of lava rock or hot crushed rock. As seen in Soza Canyon wash bank, 2% of rock has platy fractures as if conforming to margins of lava flow core, and is not brecciated. All three features support the interpretation of a volcanogenic origin for these rocks (not rock-avalanche breccia as interpreted by Dickinson and Shafiqullah, 1989, and Dickinson, 1991). This rock unit yielded a K-Ar date of 25.5 ± 0.6 Ma from groundmass feldspar (Dickinson and Shafiqullah, 1989, sample UAKA 83-75, Spencer et al., 2009c).

Tcg - Conglomerate (Miocene) - Generally poorly to moderately bedded and poorly sorted conglomerate with bed dips of 10° to 50° . This unit was included within the Paige Gravels by Lingrey (1982), which is considered equivalent to the more extensive San Manuel Formation (Dickinson, 1987, 1991), but it is possible that some of this conglomerate could be equivalent to the conglomerate at the base of the Mineta Formation (Dickinson and Olivares, 1987; Dickinson, 1991). Near the northeastern corner of the quadrangle, this unit consists of massive to poorly bedded and poorly sorted conglomerate with subrounded, 2-100 cm clasts. Up to ~90% of clasts consist of Johnny Lyon granodiorite, with sparse to locally dominant Paleozoic quartzite and carbonate. At one locality, boulders of Johnny Lyon granodiorite are up to 5 m diameter (station JES-07-513, Spencer et al., 2009a).

Trx - Rhyolite intrusion and intrusive breccia - At the south edge of the map area, this unit consists of crystal-poor, massive to flow-banded rhyolite and clast-supported brecciated rhyolite. This unit is more widely exposed to the south in the adjacent Mammoth 7 1/2' Quadrangle where it is largely or entirely intrusive and includes abundant breccias consisting of angular rhyolite clasts and clasts derived from host Cloudburst Volcanics and Oracle Granite (Creasey, 1965; Gootee et al., DGM-66, Spencer et al., 2009b).

Ta - Basaltic andesite lava (Oligocene to lower Miocene) - Lava flows and autobreccia with 1-10%, generally <5 mm pyroxene and up to 10%, <6 mm, plagioclase phenocrysts. Matrix commonly contains abundant <0.1 mm plagioclase needles and equant magnetite. Oxidative alteration is typically significant to strong, and the presence of olivine was not established, although it could be present but obscured by alteration (Young et al., 2009).

Ta - Apsey Conglomerate Member - Cliff-forming, thin-bedded, yellowish- to light-gray conglomerate and some conglomeratic tuff composed of pebbles, cobbles, and scattered boulders, largely derived from the rhyolite-obsidian member. It also contains sparse to abundant fragments of older rocks, including older members of the Galiuro Volcanics. The

well-indurated, sandy, mostly noncalcareous matrix consists of quartz, feldspar, and many small rock and crystal fragments. Pumice shards and lapilli are common in some of the conglomerate, especially in the lower part. The member is well jointed and locally it erodes to conical forms and weird columnar shapes; many cliff faces are cavernous. The conglomerate conformably and gradationally overlies the "Hells Half Acre Tuff Member (Krieger, 1968a).

Th - Hell Hole Conglomerate - Well-indurated buff conglomerate, locally strongly deformed, along northeast flank of Galiuro Mountains. Composed mainly of volcanic debris; includes few beds of tuff and ash (Simons, 1964).

Thh - Hells Half Acre Tuff member - Consists of three units, from top to bottom: (1) (0-100 ft or more). Cliff- and slope-forming, white, air-fall and partly reworked vitric, lithic (rhyolite and pumice lapilli), and crystal tuff. Narrow, deep crevices have developed along prominent northeast- and northwest-trending joints, especially on Hells Half Acre. (2) (0-400 ft, maximum thickness between Javalina and Cave Canyons). Massive, cliff-forming, white, vitric tuff, possibly one or more nonwelded to slightly welded ash-flow tuffs. Composed of white to yellowish-brown pumice lapilli, some obsidian and rhyolite lapilli, and grains of quartz, feldspar and minor biotite. (3) (0-50 ft). Well-bedded, cliff-forming, porous, yellowish-brown to brown, finely crystalline rhyolite tuff with pumice lapilli, grains of quartz, feldspar, and biotite, and scattered accidental fragments. The base in Horse Camp Canyon is a thin wedge of crossbedded, tuffaceous sandstone. Rhyolite tuff in the northeast corner of the quadrangle is tentatively included in this member, although some of it is overlain by the rhyolite-obsidian member. Pumice lapilli and groundmass of the member have been extensively zeolitized (heulandite or clinoptilolite). Equivalent to Tgut unit in Simons 1964 USGS Professional Paper 461 (Krieger, 1968a).

Tro - Hells Half Acre Rhyolite-obsidian - Gray and black, flow-banded to massive, perlitic to lithophysal obsidian, finely laminated to contorted, gray, stony (devitrified), locally lithophysal rhyolite, flow breccias. Some breccias are composed of angular fragments of very vesicular, vitric rhyolite. Rhyolite and obsidian contain small amounts of sanidine, quartz, plagioclase, pyroxene, hornblende, iron oxide, and sphene, and scattered accidental fragments. Lithophysae, generally 1-3 cm in diameter, in places are strung out, giving large outcrops a steeply dipping, bedded appearance. Chalcedony-lined geodes are as much as 10 cm in diameter. The member probably was extruded as domes and stubby flows. Cinder cones, some unmapped, consist of steeply dipping, well-bedded material, associated with tuff, conglomerate, and breccia. They contain variable amounts of older rocks (Krieger, 1968a).

Tuav - Virgus Canyon upper Andesite - Dark-colored, fine-grained, amygdaloidal andesite with small phenocrysts of plagioclase, altered olivine, and pyroxene. Exposed only as thin flows along Aravaipa and Virgus Canyons upstream from their junction, and as a thin remnant (?) south-southwest of the mouth of Javalina Canyon. Overlain by the rhyolite-obsidian member in Horse Camp Canyon. Mapped as upper andesite unit by Simons (1964), who correlated it with andesite that overlies rhyolite-obsidian north of Aravaipa Canyon, in an area where his upper tuff unit (Hells Half Acre Tuff Member) is absent. Equivalent to Tgua unit in Simons 1964 USGS Professional Paper 461 (Krieger, 1968a).

Tcv - Virgus Canyon Conglomerate - Pebbles and cobbles derived from lower andesite of Virgus Canyon and older rocks in a sandy matrix. Along Whitewash, Bear Springs, and lower Aravaipa Canyons, 0-25 ft of unmapped conglomerate composed largely of the lower andesite separates the Aravaipa Member from the Hells Half Acre Tuff Member. A few feet of unmapped conglomerate locally underlies the lower andesite (Krieger, 1968a).

Tlav - Virgus Canyon lower Andesite - Medium-gray, light-brown-weathering, very coarsely porphyritic andesite (the so-called turkey-track porphyry of Cooper, 1961) with platelike plagioclase as much as 2 cm long and 0.2 cm thick; small (mostly less than 1 mm) olivine(?) altered to orange iddingsite (bowlingite?), and minor clinopyroxene in a groundmass of plagioclase laths, clinopyroxene, iron ore, altered olivine, and apatite needles. Some andesite has only small olivine and 2-3 mm plagioclase phenocrysts. Staining with cobaltinitrite reveals some potassium feldspar in the groundmass. Equivalent to Tgia unit in Simons 1964 USGS Professional Paper 461 (Krieger, 1968a).

Taru - Aravaipa Member, nonwelded zone - Massive, slope-forming white tuff, characterized by devitrification and vapor-phase crystallization. Equivalent to Tguw unit in Simons 1964 USGS Professional Paper 461 (Krieger, 1968a).

Tar - Aravaipa Member, welded zones - Partly welded, welded, and lower nonwelded zones (200-250 ft in most places). Largely cliff-forming and consisting of, from top to bottom: (1) Columnar-jointed, vapor-phase zone (0-80 ft, thickest in Aravaipa Canyon). Very light shades of gray and brownish-gray, slightly welded, devitrified tuff with vapor-phase crystallization pronounced in pumice lapilli. (2) Welded, devitrified zone (0-160 ft). Light shades of brown and red, mostly dark-weathering tuff that becomes darker colored and densely welded downward. Some vapor-phase crystallization in pumice lapilli in upper part. Thoroughly devitrified, becoming less so near base. The lower two-thirds is characterized by large vugs and silica-lined or filled lithophysae (the "vuggy" zone). (3) Thoroughly welded zone (0-30 ft). Black and dark-brownish-gray vitrophyre with local brown oxidized lenses and devitrified spots. (4) Lower nonwelded zone (0-10 ft). Grayish-orange-pink vitric tuff, becoming lighter colored to nearly white at base. The distal end of the flow is exposed

intermittently in canyon walls from Bear Springs to Cave Canyons and the change from welded to nonwelded tuff completely exposed along lower White Wash Canyon. Equivalent to Tguw unit in Simons 1964 USGS Professional Paper 461 (Krieger, 1968a).

Tcb - Bear Springs Canyon Conglomerate - Includes conglomerate above and below the tuff (Ttb). Above the tuff (0-25 ft), fragments are Paleozoic rocks and older members of the Galiuro Volcanics. Below the tuff, fragments are largely andesite and diabase (Krieger, 1968a).

Ttb - Bear Springs Canyon Tuff - Rhyolitic ash-flow tuff composed of pumice lapilli, crystal and some accidental fragments. Upper part, where remnant, is columnar-jointed to very light-olive-and brownish-gray, partly welded tuff showing vapor-phase crystallization and containing local lithophysae near base. Lower part is moderate-orange-pink poorly welded tuff, grading down into light-colored nonwelded vitric tuff with slight clay alteration (Krieger, 1968a).

Tcd - Conglomerate of Depression Canyon - Composed of older rocks, including older members of the Galiuro Volcanics. In the northwest part it includes material from the Late Cretaceous and (or) early Tertiary volcanic and intrusive rocks (Krieger, 1968a).

Tad - Depression Canyon Andesite - Tertiary basalt and andesite of Willden, 1964. Massive, flow-banded, to agglomeratic, gray, brown, and olive andesite that weathers to lighter shades of brown. Local tuff and breccia beds are at base and between flows. The vesicular, nonvesicular, or amygdaloidal andesite contains a few to abundant, mostly small phenocrysts of plagioclase, olivine (altered or partly altered to iddingsite, rarely to serpentine), pyroxene, and magnetite. The groundmass consists of plagioclase microlites, pyroxene, iddingsite, magnetite, and some K-feldspar. The presence of isolated thin beds of rhyolite tuff suggests that thicker sections may include upper andesite of Virgus Canyon, or younger andesites (Krieger, 1968a).

Thj - Holy Joe Member - Quartz-latitude ash-flow tuff. Largely black and brown vitrophyre, composed of abundant crystal fragments (quartz, plagioclase, biotite, and sanidine), pumice lapilli, and accidental fragments in a firmly welded shard matrix; nonwelded at base, upper part slightly devitrified, except where overlain by a thin vitrophyre. South of the quadrangle (Krieger, 1968b) the member is 200-300 ft thick and forms a single cooling unit composed of several flows, the top flow being a vitrophyre (Krieger, 1968a).

Tw - Whitetail(?) Conglomerate - Composed of pebbles and cobbles of Precambrian and Paleozoic rocks, largely diabase, quartzite, and limestone. It includes a bed of white rhyolite tuff (0-25 ft thick) in Aravaipa Canyon and below the tuff a small mass of andesite

(unmapped) on the north side of the creek about 0.7 mile northeast of Wagner Ranch (Krieger, 1968a).

Twt - Rhyolite tuff bed within Whitetail Conglomerate - White rhyolite tuff bed (0-25 ft thick) in Aravaipa Canyon (Krieger, 1968a).

Tg - Conglomerate (Cenozoic) - Tan, thin- to medium-bedded, pebble-cobble, sandy matrix conglomerate and pebbly sandstone dominated by angular to sub-rounded clasts of Uncle Sam Tuff, and porphyry of Fairbank. The sandy matrix consists of quartz, feldspar, lithic grains, and 5-10% heavy and opaque minerals (Hayes and Raup, 1968).

TKm - Mafic dikes (Cenozoic-Cretaceous) - Fine-grained, crystalline matrix porphyry dikes, containing 1-5%, 1-2.5mm melt inclusion-rich plagioclase, 1-3% 1mm clinopyroxene, and 5% 1-3mm strongly altered grains (Spencer et al., 2009c).

TKh - Horse Mountain Volcanics - Silicic lava, tuff, welded tuff, obsidian, and vitrophyre; subordinate andesite and dacite. Lenticular conglomerate at base, locally fossiliferous. Numerous necks and vent breccias. Southwest flank of Santa Teresa and Turnbull Mountains (Simons, 1964).

Kai - Fine-grained andesite dikes (Cretaceous) - Andesite dikes containing <5%, <1mm plagioclase phenocrysts in very fine-grained matrix (Pearthree et al., 2009b).

Kg - Quartz monzonite of Bronco Hill (Upper Cretaceous) - Medium-grained, slightly plagioclase-porphyrific, 10% biotite-hornblende, quartz monzonite to quartz monzodiorite. The quartz monzonite contains 1-10%, 1-10cm, rounded irregular fine-grained dioritic inclusions. Marvin and Cole (1978) report a K/Ar biotite age of 76.30 ± 1.80 Ma for this unit (Pearthree et al., 2009b).

Kbi - Basaltic dikes (Cenozoic-Cretaceous) - Fine-grained basaltic dikes containing 1-2% >1.5mm plagioclase phenocrysts in a fine-grained crystalline matrix with aligned plagioclase microlites (Ferguson et al., 2009).

Krd - Porphyry of Fairbank (Upper Cretaceous) - Phenocryst-rich porphyry containing 25-40% phenocrysts of plagioclase (0.5-5.0mm), potassium feldspar (0.5-3.0mm), quartz (0.5-5mm), biotite (0.5-2.5mm), and 1-10%, 1-10cm, rounded irregular, fine-grained dioritic inclusions. The porphyry, although containing a phenocryst assemblage essentially identical to the Uncle Sam Tuff, can be distinguished from the tuff by a slightly coarser grained, more evenly distributed porphyritic texture, and the lack of pumice and lithic lapilli. The porphyry of Fairbank displays flow-foliation along its intrusive contacts in some areas, and north of the

town of Fairbank, locally has a dark vitric matrix along intrusive contact zones. Usually, however, the matrix is crystalline, and crumbly. To the south an extensive network of laccolith shaped sills and dikes intrude the Uncle Sam Tuff northeast of the Charleston Lead Mine. The porphyry in this area is also characteristically hematite stained, and argillic altered along contacts, and forms recessive slopes and valleys between the more resistant, dark-colored steep hills and knobs of the Uncle Sam Tuff (Ferguson et al., 2009).

Kgs - Quartz monzonite of Government Draw (Upper Cretaceous) - Medium-grained, slightly plagioclase-porphyritic, 10% biotite-hornblende, quartz monzonite. The quartz monzonite contains 1-10%, 1-10cm, rounded irregular fine-grained dioritic inclusions and is very similar to the quartz monzonite of Bronco Hill and the Schefflien Granodiorite. The quartz monzonite of Government Draw is distinguished by its location, by a contact phase that is very similar to the coarse-grained andesite porphyry dikes mapped just north of this quadrangle, and because it contains locally abundant fine- to medium-grained leucogranite dikes. The quartz monzonite of Government Draw is probably the youngest pluton in the area because coarse-grained andesite porphyry dikes that appear to be derived from it intrude the other plutons (Pearthree et al., 2009b).

Ku - Uncle Sam Tuff (Upper Cretaceous) - Phenocryst-rich ash-flow tuff containing 25-40% phenocrysts of plagioclase (0.5-3.0mm), sanidine (0.5-2.0mm), quartz (0.5-5mm), and biotite (0.5-2.5mm). Lithic lapilli (1-25%) consist chiefly of andesite and rhyolitic volcanics, sandstone, and argillite. Pumice lapilli, rarely significantly compacted, make up between 1 and 20% of the tuff. The pumice lapilli contain similar phenocrysts as in the tuff matrix, but the phenocrysts are slightly larger, more euhedral, and display a more evenly distributed texture. The tuff also contains 1-10%, 1-10cm, rounded, irregular, fine-grained dioritic inclusions. Most of the dioritic inclusions are not believed to be exotic lithic fragments because the same inclusions (in roughly the same abundance, and size range) are found in the porphyry of Fairbank (Krd), the quartz monzonite of Bronco Hill, and a distinctive swarm of coarse-grained, andesite porphyry dikes (Kad). The tuff is typically dark gray with a very fine-grained crystalline to vitric matrix and is usually resistant, forming steep rounded hills and knobs. To the north, the tuff includes extensive zones of megabreccia which are typically less resistant, forming slopes and low areas. Clasts in the megabreccia are similar to those seen elsewhere in the tuff, but also include zones of carbonate clasts in the northeast. Marvin et al. (1973) report a K/Ar biotite age of 73.5 ± 2.80 Ma for this unit from a sample along the western edge of the map area (Ferguson et al., 2009).

Kux - Uncle Sam Tuff megabreccia - Zones of megabreccia within the Uncle Sam Tuff. Clasts of andesite and rhyolitic volcanics, sandstone, argillite, and carbonate range in size from 1cm to several meters (Ferguson et al., 2009).

Kuxa - Uncle Sam Tuff andesite megabreccia - Zones of monolithic, andesite lava megabreccia within the Uncle Sam Tuff. Clasts range in size from 1cm to several meters (Ferguson et al., 2009).

Kdx - Coarse-grained andesite (Cretaceous) - FairBank: A volcanic complex dominated by coarse-grained, phenocryst-rich andesitic lava and probable hypabyssal bodies containing 15-30% 1-4 mm plagioclase phenocrysts, 1-5% 1-3 mm pyroxene phenocrysts, and sparse opaques and altered mafics. The unit consists of amalgamated lava flows and welded ash-flow tuff units of similar composition. To the north a series of gently northwest-dipping basaltic and basaltic andesite lava flows are interbedded with bedded pyroclastic and volcaniclastic sedimentary units (Ferguson et al., 2009).

Kr - Rhyolite (Cretaceous) - Rhyolite, probably chiefly a hypabyssal body, containing 5-10% 1-2.5mm quartz and feldspar phenocrysts. This unit is dominated by two large, massive, flow-foliated bodies to the south of the Charleston Lead Mine. This rhyolite is distinguished from the aphyric rhyolite (Kra) because it contains at least 5% quartz and feldspar phenocrysts (Ferguson et al., 2009).

Krt - Nonwelded ash-flow tuff (Cretaceous) - Felsic, nonwelded, thin- to thick-bedded lithic lapilli-rich ash-flow tuff and ash-fall tuff (Ferguson et al., 2009).

Kam - Medium-grained andesite dikes (Cretaceous) - North to northwest-striking, generally steeply dipping andesite dikes containing 10-20% 1-3mm euhedral plagioclase phenocrysts and lesser amounts of altered <2mm mafic phenocrysts (Ferguson et al., 2009).

Kt - Tuff of Charleston (Cretaceous) - Rhyolite ash-flow tuff containing 5-10%, 1-2.5mm quartz (2-5%), feldspar (2-5%), and biotite (<1%) phenocrysts, and 1-25% lithic lapilli composed chiefly of andesite lava, sandstone, and argillite. The tuff displays a well-developed eutaxitic foliation throughout its outcrop area. To the east, the tuff includes extensive zones of megabreccia (Ktx) dominated by clasts of andesite lava, pebble conglomerate, sandstone, and argillite (Ferguson et al., 2009).

Ktx - Tuff of Charleston megabreccia (Cretaceous) - Zones of the tuff of Charleston containing greater than 25% lithic blocks ranging in size from lapilli to greater than 50m. Lithic blocks are dominated by andesite lava, in particular blocks that consist of mixed zones of fine-grained phenocryst-poor, phenocryst-rich, and medium-grained, moderately phenocryst-rich lava. Blocks of rounded to well-rounded quartzite-clast, sandy matrix conglomerate are also fairly abundant. Much of the megabreccia unit is clast-supported, with very sparse zones of phenocryst-poor, quartz-feldspar-biotite phenocryst rhyolite tuff matrix (Ferguson et al., 2009).

Kra - Aphyric rhyolite (Cretaceous) - Aphyric to very phenocryst-poor rhyolite lava with probable zones of hypabyssal rock, and tuff breccia. The unit is typically strongly argillic altered, and is identified as lava in most areas because the unit is dominated by monolithic, angular, clast-supported breccia interpreted as autobreccia. At the western edge of its outcrop area, the aphyric rhyolite is in sharp contact with strongly argillic altered quartz monzonite of Bronco Hill, and the contact appears to be intrusive. Much of the unit in this area consists of heterolithic tuff breccia dominated by clasts of andesite lava, but sparse clasts of medium-grained quartz monzonite similar to the quartz monzonite of Bronco Hill are also present (Ferguson et al., 2009).

Kap - Andesite porphyry (Cretaceous) - A distinctive, hypabyssal andesite porphyry containing 10-25%, 1-3mm, euhedral plagioclase phenocrysts in a fine-grained crystalline matrix. Altered biotite phenocrysts (<1.5mm) comprise <5% of the rock. The porphyry also contains 1-10%, 1-10cm, rounded, irregular, fine-grained dioritic inclusions (Pearthree et al., 2009b).

Ka - Andesite (Cretaceous) - Amalgamated, andesite lava flows intruded by a myriad of dikes characterized by relatively fine-grained (<3.0mm and usually <2.0mm), euhedral to subhedral plagioclase phenocrysts. The andesite is pervasively propylitically altered with abundant epidote coated fractures and veinlets. Plagioclase phenocrysts ranging in size from <1mm to 3mm are present in abundances ranging from 1% to 30%. In most flows plagioclase phenocrysts are consistent in terms of size and abundance, but heterogenous zones are also present that probably represent andesite flows intruded by complex dike networks. Locally, lava flows are separated by thin sequences of mafic volcanoclastic sandstone, pebble conglomerate and pyroclastic rocks. Measurements of bedding in this map unit are from these thin sequences (Ferguson et al., 2009).

Ks - Bisbee Group (Lower Cretaceous) - Complexly intertonguing sequences of thin- to thick-bedded, cross-stratified and plane-bedded, quartz sandstone, feldspathic quartz sandstone, and lithic-feldspathic quartz sandstone, gray-green to red siltstone, mudstone, silty mudstone and shale, locally with abundant calcareous nodules and irregularly thin- to medium-bedded, discontinuous impure limestone, and limestone pebble conglomerate. Sparse, clast-supported and matrix-supported, medium- to thick-bedded sandy matrix, rounded to well-rounded, pebble-cobble conglomerate beds are also present. Clasts in the conglomerate consists of quartzite, argillite, vein quartz, with sparse granitoid, limestone, and felsic volcanics (Pearthree et al., 2009b).

Kl - Mural Limestone (Lower Cretaceous) - Thin- to medium-bedded, micrite, molluscan skeletal wackstone, and algal-laminated limestone interbedded with subordinate dark shale.

Sparse, medium-bedded intraclastic limestone conglomerate beds are also present. Slump folds and related soft-sediment deformation features are common (Shipman et al., 2009).

KJb - Bisbee Group, undivided (Cretaceous to Jurassic) - Carbonate, siltstone, sandstone, and conglomerate of the Bisbee Group, undivided. Much of the exposures of this unit, which form the footwall block of a thrust fault and part of the hanging-wall block of the San Pedro detachment fault, were mapped and described by Lingrey (1982) as consisting almost entirely of poorly bedded to massive, matrix-supported, cobble to boulder conglomerate with less abundant light brown, calcite-cemented, quartzose sandstone and red shale with local cross bedding and scour and fill structures. The unit is lithified but not obviously metamorphosed. Clasts were derived largely from upper Paleozoic carbonates and, less commonly, quartzites. The matrix consists largely of sands well cemented by carbonate (Lingrey, 1982). This unit was not included with the Glance Conglomerate because large areas mapped by JES and SMR consist of sandstone with little or no conglomerate (Spencer et al., 2009c).

Jtrm - Volcanic and sedimentary rocks of Mustang Mountain - Mapped and described by Hayes and Raup (1968): Siliceous flows and minor welded tuff; rhyolitic flows brownish-red to pale gray and grayish orange and locally porphyritic; flow banding common in some flows; welded tuff commonly coarse grained and quartzose; as much as 500 feet thick.

Jtrms - Volcanic and sedimentary rocks of Mustang Mountain - Mapped and described by Hayes and Raup (1968): Conglomerate, sandstone, siltstone, mudstone, and volcanic rocks. Conglomerate of limestone and chert clasts and (or) pale-red to light-brown sandstone, siltstone, and moderate-red mudstone. Locally contains rhyolitic and latitic flows (?) and tuff; 0 to more than 600 feet thick.

Pcn - Concha limestone - Mapped and described by Hayes and Raup (1968): Light-gray relatively thick-bedded limestone with abundant distinctive chert nodules in many beds. Several hundred feet thick in Huachuca Mountains; as much as 570 feet thick in Mustang Mountains.

Ps - Scherrer Formation - Mapped and described by Hayes and Raup (1968): Variably resistant quartzose sandstone and medium-gray dolomite about 550 feet thick; upper and lower of three members stippled on map where formation is subdivided north of the San Ignacio del Babocomari Grant. Upper member quartzose sandstone, nearly white to yellowish-gray, thinly laminated and cross-laminated; about 100 feet thick. Middle member carbonate, largely medium-gray thin- to medium-bedded dolomite; quartz nodules common; chert nodules locally abundant; about 150 thick. Lower member light-brown quartzose sandstone,

laminated to thin bedded, locally cross laminated; medium-gray dolomite beds toward base; moderate-red mudstone at base; about 300 feet thick.

Pe - Epitaph dolomite - Mapped and described by Hayes and Raup (1968): Dolomite and limestone, marl, siltstone, and gypsum about 860 feet thick; middle of three members stippled on map north of San Ignacio del Babocomari Grant. Upper member medium-to dark-gray medium-to thick-bedded resistant dolomite and limestone; chert and quartz nodules locally common; about 280 feet thick. Middle member yellowish-gray to pale-pink marl, siltstone, and argillaceous dolomite; locally contains beds of gypsum; about 450 feet thick. Lower member medium-and dark-gray to brownish-gray medium- to thin-bedded dolomite; about 130 feet thick.

Pc - Colina limestone - Mapped and described by Hayes and Raup (1968): Medium-to dark-gray limestone. As much as 175 feet of dark-gray dolomite of the Epitaph Dolomite locally mapped with the Colina in the Huachuca Mountains; total mapped unit about 1,050 feet thick. Colina about 350 feet thick in Mustang Mountains.

PIPet - Tectonite derived from Earp Formation (Pennsylvanian to Permian protolith) - Generally consists of medium to light gray limestone, silty limestone, sandy limestone, and beds of quartzite (Spencer et al., 2009a).

PIPeht - Tectonite derived from Horquilla Limestone and Earp Formation, undivided (Pennsylvanian to Permian protolith) - Interbedded marble and calc-silicate gneiss (Lingrey, 1982).

IPhMet - Marble tectonite derived from Horquilla Limestone and Escabrosa Limestone, undivided (Mississippian to Pennsylvanian protolith) - Typically calcite marble and slightly siliceous calcite marble (mapped by Lingrey, 1982).

Mzs - Clastic sedimentary rocks - Sandstone and siltstone with basal conglomerate and chert-fragment breccia. The basal part of this unit consists of a 5-10-m-thick, chert-clast breccia to angular-clast conglomerate. Clasts are 1-10 cm diameter, angular, and composed of fine-grained quartzose rocks (chert). Some clasts contain fossil debris, some with radial, coral-like form as if derived from underlying Paleozoic carbonates. Just above basal contact, chert-clast breccia forms 50-200-cm-thick beds, interbedded with similar-thickness sandstone that is pale gray, tan, or reddish tan. Above basal breccia and conglomerate, rocks of this unit consist of plane-bedded, reddish brown, medium-grained sandstone. Upper part of unit consists of friable, very fine-grained quartzose sandstone to siltstone. This unit was mapped by Krieger as thrust over underlying Escabrosa Limestone (Krieger, 1968d). However, this thrust contact is interpreted as depositional based on new mapping (Spencer and Richard,

2008), with a basal chert-clast breccia derived from weathering of underlying Escabrosa Limestone and possibly other Paleozoic carbonate units (Young et al., 2009).

Me - Escabrosa Limestone - Massive, cliff-forming, thick-bedded, mostly coarsegrained, limestone in shades of gray and yellowish to greenish gray. The cliffs, as much as 50 ft high, are separated by narrow slopes of thin-bedded, medium- to fine-grained gray limestone and brown silty and dolomitic limestone. Chert nodules are common in some beds, especially in upper part. The basal part is crossbedded, coarse-grained brown sandstone and dolomitic sandstone (0-10 ft) overlain by limestone that resembles beds near the top of the Martin Formation. Fossils are abundant and include crinoids, brachiopods, and corals, and in the upper part many ostracodes. Dark-brown chert breccia, common in some areas, may represent pre-Naco solution and erosion (Krieger, 1968a).

Dm - Martin Formation - A slope-forming shale unit generally with overlying and thinner underlying carbonate beds. The shale is olive to reddish brown, with interbedded reddish-brown and light-brownish-gray limestone beds (2 in. to 4 ft thick) in the upper part. These limestone beds weather to rounded surfaces that are light shades of brown and red. The top in thicker sections consists of coarse-grained, light-gray Escabrosa-like limestone. Brachiopods, bryozoa, and crinoids are common in the limestone beds. The shale may rest directly on the Abrigo Formation, or be separated from it by as much as 25 ft of very fine grained, pale-reddish-brown or light-gray, medium-grained limestone. The base is generally a few inches of hematite-rich sandstone with granules and small pebbles of quartz and abundant shark teeth and arthro-diran fish fragments. The hematitic beds occur at the same horizon as the oolitic hematite bed on the Christmas quadrangle (Willden, 1960,1964, Krieger, 1968a).

€au - Abrigo Formation, upper member - Brown sandy member (116-165 ft). The Upper part (70-100 ft) is slope-forming, thin-bedded (Vz-1 ft, locally 2 ft), medium- to coarse-grained dolomite and dolomitic sandstone in light shades of brown. It contains some argillaceous and glauconitic beds, intraformational conglomerate, irregular surficial chert, and a few thin chert beds and lenses. Silicified specimens of the brachiopod *Billingsella* occur in a narrow horizon near the middle of thicker sections. The lower part (75-95 ft) is cliff-forming, dark-brown-weathering, thin to thick-bedded (8 in. to 8 ft, mostly 3 ft), mostly poorly sorted and cross-bedded, dolomitic and glauconitic sandstone; some dolomite, sandy and glauconitic dolomite, light-colored sandstone and quartzite, intraformational conglomerate, and siltstone; local granule and small-pebble conglomerate beds. Phosphatic brachiopod scraps are generally abundant in the dark-brown-weathering beds. Fucoids and *Scolithus* occur in light-colored sandstones (Krieger, 1968a).

€am - Abrigo Formation, middle member - Middle (sandstone) member (about 270 ft).- Predominantly cliff-forming, yellowish-gray, thin- to thick-bedded (3 in. to 3 ft), mostly

poorly sorted sandstone, and argillaceous sandstone; some granule conglomerate and thin to very thin silty or shaly partings. Most bedding surfaces are irregular due largely to abundant fucoids. Scolithus also are generally abundant. The upper part contains local beds of pronounced, steep crossbedding and 2- to 6-in. beds of white quartzite. Locally in the lower part a 10- to 40-ft massive unit has smooth bedding surfaces, no fossils, and only sparse shaly partings; it is overlain by 2-30 ft of mudstone-siltstone beds like those in the lower member. Contact with the lower member is arbitrarily located in some places and is not everywhere at the same horizon, partly because of variations in influx of sand in the upper part of the lower member (Krieger, 1968a).

€al - Abrigo Formation, lower member - Mudstone member (0- about 155 ft).- A thin-bedded, slope-forming, poorly sorted, argillaceous and sandy unit that weathers to shades of brown and yellowish to reddish brown. It consists of massive to very thin bedded (1/2-2 in.), in part thinly laminated, olive- to greenish-gray, and grayish-red mudstone, siltstone, and sandy mudstone; interbedded argillaceous sandstone beds (1 in. to 1 and locally 3 ft) and thin (mostly about 1 in.), well-sorted, light-colored quartzite and sandstone beds, paper-thin shale, and local beds and lenses of granule to small-pebble conglomerate. The member becomes more sandy and lighter colored upward. Most bedding surfaces are extremely irregular and pellety. Phosphatic brachiopod scraps are generally abundant; fucoids and Scolithus are present, but are mostly smaller and less abundant than in the middle member. Where the formation rests on diabase the base generally is a conglomerate (0-50 ft) composed of cobbles to small boulders (largely Troy Quartzite) in a grayish-red, sandy, diabasic matrix. Overlying beds commonly contain dolomite as cement, or as layers, lenses, nodules, and detrital pebbles (Krieger, 1968a).

€a - Abrigo Formation - Divided into three units by Krieger (1968c), but field mapping by Spencer and Richard resulted in correlation of the middle and lower units with the Cambrian Bolsa Quartzite, which was not identified by Krieger in the Lookout Mountain Quadrangle. The Abrigo Formation consists of thin- to thick-bedded, cross bedded, dolomitic sandstone with local dolomite, siltstone, sandstone, and intraformational conglomerate (upper unit of Krieger, 1968c). Dark chocolate-brown calcareous sandstone is characteristic of this unit in easternmost exposures (Young et al., 2009).

€b - Bolsa Quartzite - Fine- to locally medium-grained sandstone, plane bedded to cross bedded. Sandstone varies from chocolate brown to orangish tan to white. Sandstone is coarse to granule within basal several meters. Pebbly beds with quartzite pebbles up to 3 cm are present locally near the base. Locally abundant, cylindrical trace fossils (burrows?), <1 cm diameter, visible on both on bedding planes and on surfaces perpendicular to bedding planes, indicate that this unit is not Proterozoic. Lack of carbonate and coarseness indicate correlation with Bolsa Quartzite rather than Abrigo Formation (Young et al., 2009).

Xgj - Johnny Lyon granodiorite (Paleoproterozoic) - Medium-grained biotite granodiorite with blocky, 1-4 cm long, K-feldspar megacrysts that make up 10-25% of the rock unit, and ~5-10% mafic minerals, most of which is probably biotite but is generally too altered for definitive identification. On the north side of Wildhorse Mountain, within a few hundred meters of the trace of the Wildhorse Mountain thrust fault, K-feldspar phenocrysts are generally 5-12 mm diameter, and gray quartz phenocrysts (up to at least 6 mm) are conspicuous. Possibly this is due to alteration near the thrust, or to proximity to the San Pedro detachment, or it could be due to primary textural variations within the granodiorite. Two modal mineral analyses by Cooper and Silver (1964), from samples east of the map area in the Johnny Lyon Hills, determined that the unit is a granodiorite.

Xdj - Dioritic rocks associated with Johnny Lyon granodiorite (Paleoproterozoic) - Dark colored, mafic rich dioritic rock that forms local, small irregular bodies in Johnny Lyon Granodiorite. Texturally similar to non-porphyrific parts of Johnny Lyon Granodiorite Spencer et al., 2009a).

Yd - Diabase - Dark greenish gray to olive gray, medium grained diabase forming sills and dikes in all Proterozoic rock units. Krieger (1968b) described the diabase as ophitic and consisting of 3-5 mm plagioclase, pyroxene (some poikilitic crystals as large as 1 cm), magnetite, ilmenite, and sparse olivine. This unit is correlated with the Sierra Ancha diabase (Wrucke, 1989, Young et al., 2009).

db - Diabase - Dark-gray to dark-greenish or olive-gray, medium-grained diabase occurring mostly as sills and multiple sills (totaling more than 1,000 ft in places). The texture is diabasic, ophitic, or poikilitic. The rock contains plagioclase (mostly about 5 mm, locally 2 cm), smaller pyroxene (poikilitic crystals are as much as 2 cm across), magnetite, ilmenite, and minor olivine. Some thicker sills contain aplitic and pegmatitic differentiates. The chilled contact of diabase against older rocks (including earlier sills) contrasts with the weathered appearance of diabase beneath Paleozoic rocks, where, within a zone as much as 20 ft thick, diabase grades upward from fresh, massive, dark-gray rock into crumbly, red to purple rock with a pronounced platy structure (Krieger 1968a, 1968b).

tu - Troy Quartzite, upper unit - White to very light gray, locally grayish-red, somewhat lenticular, thin to thick-bedded (mostly 1-3 ft), feldspathic (white feldspar or clay alteration) to non-feldspathic sandstone, quartzite, and granule to small-pebble (less than 1/2 in.) conglomerate. Pebbles are composed largely of quartz; some are concentrated on tops of beds. The unit contains local slump structures and large-scale crossbedding. Surficial silicification obscures some bedding features (Krieger, 1968b).

- tl - Troy Quartzite, lower unit - Lower unit, dark-brownish-gray outcrops of medium-gray to pale-red conglomerate and sandstone that are mostly thin bedded (many are 6 in; or less), lenticular, and channeled. The upper part consists of light-colored sandstone and quartzite interbedded with and replaced downward by dark sandstone, granule to small-pebble conglomerate, and thin beds of greenish-gray argillite. Much of the conglomerate contains abundant pink to orange fragments of feldspar and quartz porphyry or rhyolite. The basal 30-50 ft consists of pale-red sandstone and conglomeratic sandstone, in most places metamorphosed (by diabase) to light-bluish gray, underlain by pebble to small-cobble conglomerate that locally contains sparse to closely packed, well-rounded pebbles derived from the Barnes Conglomerate Member of the Dripping Spring Quartzite (Krieger, 1968b).
- Yt - Troy Quartzite - The Troy Quartzite was divided by Krieger (1968b) into two units, as follows: (1) an upper unit (up to 200 m thick) of white to very light gray, thin- to thick-bedded feldspathic to quartzose sandstone and granule to small-pebble conglomerate, and (2) a lower unit (up to 120 m thick) of mostly thin-bedded, medium gray to pale red sandstone and granule to small pebble conglomerate (Young et al., 2009).
- ds - Dripping Springs Quartzite - Upper and Middle members, the upper member is thin-bedded (1/4 -12 in.), very fine grained, feldspathic to arkosic quartzite and siltstone that are shades of gray, brown, red, and yellow. The middle member is thin- to thick-bedded (2-12 ft), crossbedded, medium-grained, locally fine-to coarse-grained, red to pink, feldspathic to arkosic quartzite, with a little nonfeldspathic quartzite. On the north side of the large granitic mass, the few feet of quartzite above the granite contain angular quartz and granitic fragments (Krieger, 1968b).
- Yds - Dripping Spring Quartzite - This unit consists of gray, brown, red, and yellow, feldspathic, arkosic, and quartzose sandstone and less abundant siltstone. Sands are typically fine to medium grained and appear feldspathic with red K-feldspar grains. Sandstone is locally cross bedded. Bed thickness decreases upsection, from very thick bedded (locally to 4 m) near the base to thin to medium bedded (<25 cm) at higher stratigraphic levels (Krieger, 1968b, Young et al., 2009).
- Ym - Mescal Limestone - Thick to thin bedded, brown to gray dolomite and silty to cherty dolomite, less abundant laminated limestone, and brown dolomitic sandstone locally at base (Krieger, 1968b). Asbestos veins are locally present near intrusive contact with diabase. This unit appeared in easternmost exposures as silty to cherty, medium to light brown dolostone, with laminations locally in dolostone. These laminations likely would have been obliterated by bioturbation if this unit were Phanerozoic (Young et al., 2009).

Ydsb - Barnes Conglomerate Member, Dripping Spring Quartzite - Up to 4 m of pebble and cobble conglomerate, with well rounded clasts up to 12 cm diameter of quartzite, vein quartz, and red jasper, in a matrix of red to gray arkosic sandstone (Krieger, 1968b).

Yp - Pioneer Formation - Dark red to purple siltstone and fine-grained to very fine-grained sandstone, and light reddish orange fine- to medium-grained to locally coarse-grained, cross-bedded sandstone. Grain size generally decreases up section (Krieger, 1968b, Young et al., 2009).

Yo - Oracle Granite - Porphyritic, medium- to coarse-grained biotite granite ("quartz monzonite" of Krieger [1968a]). Microcline phenocrysts are as large as 2 x 4 cm and somewhat poikilitic, with included mafic minerals imparting a speckled appearance. K-feldspar is commonly pink to reddish, and mafic minerals are generally abundant (7-12%). [Speckled, poikilitic, reddish to pink K-feldspar megacrysts and abundant mafics dominated by aggregates of fine biotite are characteristic of Oracle Granite that are commonly used as criteria for tentative correlation]. Granite in the Samaniego Hills, located 70 km to the southwest and probably correlative with the Oracle Granite, yielded a U-Pb data of 1434.5 ± 3.4 Ma (Young et al., 2009).

Yoa - Oracle Granite, alaskitic - Equigranular, medium to coarse grained, dark orange to pale red alaskite that is gradational with the Oracle Granite (Krieger, 1968a). Local porphyry, aplite, and potassic granite were included with this map unit by Krieger (1968a). Fine grained, two-mica granite in the Black Mountain area to the west yielded a U-Pb data of 1433.5 ± 2 Ma (Spencer et al., 2003, Young et al., 2009).

py - Porphyry - Massive to slightly foliated, fine-grained porphyritic rock in shades of red, brown, and gray. Sparse to abundant phenocrysts of quartz and plagioclase (1 to rarely 3 mm) and scattered lithic fragments (2 cm long or more) are in a dense groundmass of quartz, alkalic feldspar, variable amounts of sericite, and some epidote, biotite, magnetite, and chlorite. The porphyry is locally cut by minute quartz veins, or by larger gash or ladderlike veins of milky quartz (Simons, 1964).

gru - Granitic rocks, undivided - Composed largely of granodiorite or nonporphyritic quartz monzonite, and some alaskite. The granodiorite or quartz monzonite is medium grained (mostly less than 5 mm), pale red to grayish orange pink with olive-gray spots. Composed of saussuritized plagioclase (a few as much as 1 cm); K-feldspar, quartz, altered hornblende and biotite, and accessory sphene, magnetite, and allanite. Texturally the rock resembles neither the porphyritic quartz monzonite or the granodiorite in the Lookout Mountain quadrangle (Krieger, 1968c). The alaskite is medium to coarse grained and orange pink to pale red and contains microcline, plagioclase, quartz, and a little biotite, muscovite, and

magnetite-chlorite alteration. Close to the pre-Apache surface the granitic rock is generally redder in color, richer in K-feldspar (in places to the exclusion of plagioclase), and poorer in mafic minerals, but this rock and the alaskite appear to grade down into the granodiorite or quartz monzonite (Krieger, 1968b).

pi - Pinal schist - Mostly flows, tuffs, and flow breccias of andesitic composition and some rhyolitic tuffs. The mafic flows and breccias are largely dark gray, greenish gray, and dusky yellow. The bedded tuffs are lighter colored, very fine grained rocks, some of which have been tightly drag folded. Most of the rock is nonschistose; locally a pencil structure has been formed by the intersection of two cleavages. The Pinal has locally been replaced by quartz and carbonate veins that contain tourmaline or pyrite, or by wide veins of dark-purplish-black quartz. North and south of Aravaipa Canyon, most of the Pinal is medium-gray to medium-light-gray, fine-grained, bedded quartz-sericite-magnetite rock with slaty cleavage. It contains some medium-dark-greenish-gray chloritic rocks, probably volcanic breccia, conglomerate, or mafic flow, and some massive pink rhyolite tuff or flow (Krieger, 1968b).

References

- Birkeland, Peter W., 1999, *Soils and Geomorphology* (3rd Ed.): Oxford University Press, New York, 429 pp.
- Bahre, C.J., 1991, *A Legacy of Change: Tucson*, University of Arizona Press, 231 p.
- Bull, W.B., 1991, *Geomorphic Response to Climatic Change*: Oxford University Press, New York, 326 p.
- Cattanach, George S., Jr., 1966, A San Pedro stage site near Fairbank, Arizona: *The Kiva*, v. 32, no. 1, p. 1-24.
- Clark, Jeffrey J., and Lyons, Patrick D., 2003, Mounds and migrants in the Classic Period (A.D. 1200-1450): *Archaeology Southwest*, v. 17, no. 3.
- Cook, J.P. and Spencer, J.E., 2009, Geologic Map of the Redington 7½' Quadrangle, Cochise, Graham, and Pima Counties, Arizona: Arizona Geological Survey Digital Geologic Map 60 (DGM-60) version 2.0, 1 sheet, layout scale 1:24,000, with text.
- Cook, J.P., Shipman, T.C., Pearthree, P.A., and Haddad, D.E., 2009, Geologic map of the Hereford 7½' Quadrangle and the Northern Part of the Stark 7½' Quadrangle, Cochise County, Arizona: Arizona Geological Survey Digital Geologic Map 57 (DGM-57), v. 2.0, 1 sheet, layout scale 1:24,000, with text.
- Cooke, R.U., and Reeves, R.W., 1976, *Arroyos and environmental change in the American South-West*: Oxford, Clarendon Press, 213 p.
- Cooper, J.R., and Silver, L.T., 1964, Geology and ore deposits of the Dragoon quadrangle, Cochise County, Arizona: U.S. Geological Survey Professional Paper 416, 196 p., 13 sheets, scales 1:600, 1:1,200, 1:2,400, 1:4,800, 1:12,000, 1:31,680, 1:125,000.
- Cordell, Linda, 1997, *Archaeology of the Southwest* (2nd Ed.): Academic Press, Inc., San Diego, 522 pp.
- Damon, Paul E., and Long, Austin, 1962, Arizona radiocarbon dates III: *Radiocarbon*, v. 4, p. 239-249.
- Demsey, K.A., and Pearthree, P.A., 1994, Surficial and environmental geology of the Sierra Vista area, Cochise County, Arizona: AZGS OFR 94-6, 14 p., scale 1:24,000.
- Dickinson, W.R., 2003, Depositional facies of the Quiburis Formation, basin fill of the San Pedro trough, southeastern Arizona Basin and Range Province, *in* Reynolds, R.G., and Flores, R.M., eds, 2003, *Cenozoic systems of the Rocky Mountain region*: Denver, Rocky Mountain Section, SEPM (Society for Sedimentary Geology), p. 157-181.
- Ferguson, C.A., Shipman, T.C., Pearthree, P.A., Moore, E.M., Richard, S.M., Spencer, J.E., Youberg, A., Cook, J.P., and Haddad, D.E., 2009, Geologic map of the Fairbank 7 ½' Quadrangle, Cochise County, Arizona: Arizona Geological Survey Digital Geologic Map 50 (DGM-50), v. 2.0, 1 sheet, layout scale 1:24,000, with text.

- Gile, L.H., Hawley, J.W., and Grossman, R.B., 1981, Soils and geomorphology in the basin and range area of southern New Mexico -- guidebook to the Desert Project: New Mexico Bureau of Mines and Mineral Resources Memoir 39, 222 p.
- Gootee, B.F., Spencer, J.E., Ferguson, C.A., Richard, S.M., Cook, J.P., and MacFarlane, B.J., 2009, Geologic map of the Clark Ranch 7½' quadrangle and the western half of the Rhodes Peak 7½' quadrangle, Pinal and Graham Counties, Arizona: Arizona Geological Survey Digital Geologic Map DGM-68, version 1.0, scale 1:24,000, 19 p. 1 sheet.
- Gray, R.S., 1965, Late Cenozoic sediments in the San Pedro Valley near St. David, Arizona: Tucson, University of Arizona, Ph.D. dissertation, 198 p, 3 sheets.
- Hastings, J.R., 1959, Vegetation change and arroyo cutting in southeastern Arizona: Arizona Academy of Science, Journal, v. 1, no. 2, p. 60-67.
- Hastings, J. R., and R. M. Turner. 1965. *The changing mile: An ecological study of vegetation change with time in the lower mile of an arid and semi-arid region*. University of Arizona Press: Tucson. 317 p.
- Hayes, P.T., and Raup, R.B., 1968, Geologic map of the Huachuca and Mustang Mountains, southeastern Arizona: U.S. Geological Survey Miscellaneous Geologic Investigations Map I-509, 1 sheet, scale 1:48,000.
- Haynes, C.V., Jr., 1966, Unpublished field notes.
- Haynes, C.V., Jr., 1987, Curry Draw, Cochise County, Arizona: A late Quaternary stratigraphic record of Pleistocene extinction and paleo-Indian activities, in Hill, M.L., ed., Cordilleran Section of the Geological Society of America: Geological Society of America, Centennial Field Guide Volume 1, p. 23-28.
- Haynes, C. Vance, Jr., 2007, Radiocarbon dating at Murray Springs and Curry Draw. In Murray Springs: A Clovis Site with Multiple Activity Areas in the San Pedro Valley, Arizona, edited by C. Vance Haynes, Jr., and Bruce B. Huckell, p. 229-239. University of Arizona Press, Tucson.
- Haynes, C. Vance, Jr., 2009, Quaternary geology of the upper San Pedro Valley. Unpublished manuscript, University of Arizona, Tucson, Arizona.
- Heckman, Robert A., Montgomery, Barbara K., and Whittlesey, Stephanie M., 2000, Prehistoric Painted Pottery of Southeastern Arizona. Technical Series 77: Statistical Research, Inc., 163 pp.
- Heindl, L.A., 1952, Upper San Pedro basin, in Halpenny and others, Ground water in the Gila River basin and adjacent areas, Arizona-A Summary: U.S. Geological Survey Open-File Report [unnumbered], p. 69-86.
- Hereford, Richard, 1993, Entrenchment and widening of the upper San Pedro River, Arizona: Geological Society of America Special Paper 282, 46 p.
- Huckell, B.B., 1990, Late Pre-ceramic Farmer-Foragers in Southeastern Arizona: A Cultural and Ecological Consideration of the Spread of Agriculture into the Arid Southwestern United States, unpublished Ph.D. dissertation, University of Arizona.

- Huckleberry, Gary, 1996, Historical channel changes on the San Pedro River, southeastern Arizona (revised October 1996): Arizona Geological Survey Open-File Report 96-15, 22 p.
- Huckleberry, G., Lite, S.J., Katz, G., and Pearthree, P.A., 2009, Fluvial Geomorphology, in Stromberg, J.C., and Tellman, B., *Ecology and Conservation of the San Pedro River*: University of Arizona Press: Tucson, p. 251-267.
- Krieger, M.H., 1968a, Geologic map of the Brandenburg Mountain quadrangle, Pinal County, Arizona: U.S. Geological Survey Geologic Quadrangle Map GQ-668, 3 p., 1 sheet, scale 1:24,000.
- Krieger, M.H., 1968b, Geologic map of the Holy Joe Peak quadrangle, Pinal County, Arizona: U.S. Geological Survey Geologic Quadrangle Map GQ-669, 4 p., 1 sheet, scale 1:24,000.
- Krieger, M.H., 1968b, Geologic map of the Lookout Mountain quadrangle, Pinal County, Arizona [Lookout Mtn. 7.5 min]: U.S. Geological Survey Geologic Quadrangle Map GQ-670, 2 p., 1 sheet, scale 1:24,000.
- Krieger, M.H., 1968c, Geologic map of the Saddle Mountain quadrangle, Pinal County, Arizona [Dudleyville 7.5 min]: U.S. Geological Survey Geologic Quadrangle Map GQ-671, 3 p., 1 sheet, scale 1:24,000.
- Lindsay, E.H., Smith, G.A., and Haynes, C.V., 1990, Late Cenozoic depositional history and geochronology, San Pedro Valley, Arizona, in Gehrels, G.E., and Spencer, J.E., eds., *Geologic excursions through the Sonoran Desert Region, Arizona and Sonora*: AZGS Special Paper 7, p. 9-19.
- Lingrey, S.H., 1982, Structural geology and tectonic evolution of the northeastern Rincon Mountains, Cochise and Pima Counties, Arizona: Tucson, University of Arizona, Ph.D. dissertation, 202 p., 5 sheets, scale 1:24,000.
- Machette, M.N., 1985, Calcic soils of the southwestern United States: in Weide, D.L., ed., *Soils and Quaternary Geology of the Southwestern United States*: Geological Society of America Special Paper 203, p. 1-21.
- Marvin, R.F., Stern, T.W., Creasey, S.C., and Mehnert, H.H., 1973, Radiometric ages of igneous rocks from Pima, Santa Cruz, and Cochise Counties, southeastern Arizona: U.S. Geological Survey Bulletin 1379, 27 p.
- Marvin, R.F., and Cole, J.C., 1978, Radiometric ages: Compilation A, U.S. Geological Survey: Isochron/West, no. 22, p. 3-14.
- McFadden, L.D., 1981, Quaternary evolution of the Canada del Oro Valley, southeastern Arizona: Arizona Geological Society Digest, v. 13, p. 13-19.
- Menges, C.M., 1981, The Sonoita Creek Basin: Implication for late Cenozoic tectonic evolution of basins and ranges in southeastern Arizona: Tucson, University of Arizona, 239 p.
- Menges, C.M., and McFadden, L.D., 1981, Evidence for a latest Miocene to Pliocene transition from Basin-Range tectonic to post-tectonic landscape evolution in southeastern Arizona, in Stone, C., and Jenney, J.P., eds., *Arizona Geological Society Digest 13*: Tucson, Arizona Geological Society, p. 151-160.

- Menges, C.M., and Pearthree, P.A., 1989, Late Cenozoic tectonism in Arizona and its impact on regional landscape evolution, *in* Jenney, J.P., and Reynolds, S.J., eds., *Geologic Evolution of Arizona*: Tucson, Arizona Geological Society, p. 649-680.
- NRCS, 2003, Soil survey of Cochise County, Arizona, Douglas-Tombstone part: USDA Natural Resources Conservation Service, 733 p.
- Onken, J., and Huckell, B.B., 1989, An inventory and assessment of potential uses for the University of Arizona Babocomari gift-deeded parcel near Huachuca City, Arizona: Tucson, Arizona State Museum, p. 35.
- Pearthree, P.A., and Youberg, A., 2009, Geologic Map of the Huachuca City 7 ½' Quadrangle, Cochise County, Arizona: Arizona Geological Survey Digital Geologic Map 36 (DGM-36) version 2.0, 1 sheet, layout scale 1:24,000, with text.
- Pearthree, P.A., Cook, J.P., Skotnicki, S.J., and Spencer, J.E., 2009a, Geologic map of the Peppersauce Wash 7½' quadrangle and part of the Kielberg Canyon 7 ½' quadrangle, Pinal and Pima Counties, Arizona: Arizona Geological Survey Digital Geologic Map DGM-69, version 1.0, 12 p., scale 1:24,000.
- Pearthree, P.A., Ferguson, C.A., Demsey, K.A., Haddad, D.E., and Cook, J.P., 2009b, Geologic map of the Lewis Springs 7 ½' quadrangle, Cochise County, Arizona: Arizona Geological Survey Digital Geologic Map 51 (DGM-51), version 2.0, 1 sheet, layout scale 1:24,000, with text.
- Pearthree, P.A., and Calvo, S.S., 1987, The Santa Rita fault zone: Evidence for large magnitude earthquakes with very long recurrence intervals in the Basin and Range province of southeastern Arizona: *Seismological Society of America, Bulletin*, v. 77, no. 1, p. 97-116.
- Richard, S.M., Shipman, T.C., Green, L., and Harris, R.C., 2007, Estimated depth to bedrock in Arizona: Arizona Geological Survey Digital Geologic Map DGM-52, v. 1.0, scale 1:1,000,000.
- Schiffer, Michael B., 1986, Radiocarbon dating and the "old wood" problem: the case of the Hohokam chronology: *Journal of Archaeological Science*, v. 13, p.13-30.
- Shipman, T.C., and Ferguson, C.A., 2003, Geologic map of the McGrew Spring 7.5' quadrangle, Cochise County, Arizona, v. 1.0, scale 1:24,000.
- Shipman, T.C., Ferguson, C.A., Cook, J.P., and Haddad, D.E., 2009, Geologic Map of the Land 7.5' Quadrangle, Cochise County, Arizona: Arizona Geological Survey Digital Geologic Map 49 (DGM-49) version 2.0, 1 sheet, layout scale 1:24,000.
- Simons, F.S., 1964, Geology of the Klondyke quadrangle, Graham and Pinal Counties, Arizona (Klondyke, Oak Grove Canyon, Cobre Grande Mtn., and Booger Canyon 7.5 min): U.S. Geological Survey Professional Paper 461, 173 p.
- Spencer, J.E., Cook, J.P., Lingrey, S.H., Richard, S.M., Ferguson, C.A. and Guynn, J.H., 2009, Geologic Map of the Wildhorse Mountain 7 ½' Quadrangle, Cochise County, Arizona: Arizona Geological Survey Digital Geologic Map 62 (DGM-62) version 2.0, 1 sheet, layout scale 1:24,000, with text.

- Spencer, J.E., Gootee, B.F., Richard, S.M., and Cook, J.P., 2009, Geologic map of the Mammoth 7½' quadrangle, Pinal County, Arizona: Arizona Geological Survey Digital Geologic Map DGM-67, version 1.0, scale 1:24,000, 1 sheet, 18 p. text.
- Spencer, J.E., Richard, S.M., Cook, J.P., Dickinson, W.R., Lingrey, S.H., and Guynn, J.H., 2009, Geologic Map of the Soza Canyon 7½' Quadrangle, Cochise and Pima Counties, Arizona: Arizona Geological Survey Digital Geologic Map 61 (DGM-61) version 2.0, 1 sheet, layout scale 1:24,000, with text.
- Thomas, David Hurst, 1979, *Archaeology*: Holt, Rinehart and Winston, New York, 510 pp.
- U.S. Geological Survey. 2008. National elevation dataset, 1/3 arc second. *Accessed at:* <http://seamless.usgs.gov/website/seamless/products/3arc.asp>
- Vice, D.H., 1974, The geology and petrography of the Babocomari Ranch area, Santa Cruz-Cochise Counties, Arizona: Tempe, Arizona State University 152 p.
- Waters, M.R., and Haynes, C.V., 2001, Late Quaternary arroyo formation and climate change in the American Southwest: *Geology* (Boulder), v. 29, no. 5, p. 399-402.
- Waters, Michael R., and Stafford, Thomas W., 2007, Redefining the age of Clovis: Implications for the peopling of the Americas: *Science*, v. 315, p. 1122-1126.
- Webb, R.H., Leake, S.A., and Turner, R.M., 2007, *the Ribbon of Green: Change in Riparian Vegetation in the Southwestern United States*. University of Arizona Press: Tucson, 461 p.
- Willden, Ronald, 1960, Sedimentary iron-formation in the Devonian Martin Formation, Christmas quadrangle, Arizona, in *Short papers in the geological sciences, Geological Survey research 1960*: U.S. Geological Survey Professional Paper 400-B, p. B21-B23.
- Willden, Ronald, 1964, Geology of the Christmas quadrangle, Gila and Pinal Counties, Arizona: U.S. Geological Survey Bulletin 1161-E, p. E1-E64, 2 sheets, scales 1:62,500 and 1:250,000.
- Wise, E.N., and Shutler, R., Jr., 1958, University of Arizona radiocarbon dates: *Science*, v. 127, p. 72-74.
- Wood, M.L., 1997, Historical channel changes along the lower San Pedro River, southeastern Arizona: Arizona Geological Survey Open-File Report 97-21, 44 p., 3 sheets, scale 1:24,000.
- Wrucke, C.T., 1989, The Middle Proterozoic Apache Group, Troy Quartzite, and associated diabase of Arizona, in Jenney, J.P., and Reynolds, S.J., eds., *Geologic evolution of Arizona: Arizona Geological Society Digest 17*, p. 239-258
- Youberg, A., Skotnicki, S.J., Ferguson, C.A., Cook, J.P., and Shipman, T.C., 2009, Geologic Map of the Benson 7½' Quadrangle, Cochise County, Arizona: Arizona Geological Survey Digital Geologic Map 34 (DGM-34) version 2.0, 1 sheet, layout scale 1:24,000.
- Youberg, A., and Cook, J.P., 2009, Geologic Map of the Saint David 7½' Quadrangle, Cochise County, Arizona: Arizona Geological Survey Digital Geologic Map 48 (DGM-48) version 2.0, 1 sheet, layout scale 1:24,000.
- Youberg, A., Spencer, J.E., Richard, S.M., and Cook, J.P., 2009, Geologic Map of the Galleta Flat East 7½' Quadrangle, Cochise County, Arizona: Arizona Geological Survey Digital Geologic Map 56 (DGM-56) version 2.0, 1 sheet, layout scale 1:24,000, with text.

Young, J.J., Spencer, J.E., MacFarlane, B.J., and Richard, S.M., 2009, Geologic map of the Lookout Mountain 7½' quadrangle, Pinal County, Arizona: Arizona Geological Survey Digital Geologic Map DGM-66, version 1.0, scale 1:24,000, 1 sheet, 13 p. text.